Preface

This thesis is the result of a study, investigating the swash zone sediment transport processes. The first part of the thesis work has taken place on the University of Queensland, in Brisbane, Australia. The second part took place in Delft at WL Delft Hydraulics and was funded by the Delft Cluster Project Coasts (03.01.03).

My special gratitude goes to Stefan Aarninkhof for his daily assistance at WL Delft Hydraulics. The author would also like to thank Marcel Stive for helping to create the opportunity for a study in Australia.

Paul de Groot

The thesis committee consists of:

Prof. dr. ir. M.J.F. Stive
Prof. dr. ir. L.C. Van Rijn
Ir. S.G.J. Aarninkhof
Ir. G. Klopman

Summary

The coastal area is a busy area, many people live in these areas or use the coastal area for recreational purposes.
The beach profile in the coastal area is continuously changing under the changing field conditions. These changes are induced by the changing sediment transports in the sea under changing field conditions. Several models have been developed to simulate and predict these changes in sediment transport and their related profile changes. However, these models fail in a region close to the shoreline, since the parameterized wave models (like Battjes Janssen, 1978) fail in this region.

In this thesis a model has been developed to compute the sediment transport rates up to zero meter water depth. This Inner Surf Zone (ISZ) sediment transport model is based on the ISZ model of Aarninkhof, 2000, which models the wave height decay and the associated flow field up to zero meter water depth.
The ISZ sediment transport model uses the energy approach of Bailard (1963;1966) for the sediment transport computations. According to Bailard the sediment transport is related to the work done by the fluid, the dissipated energy.
The sediment transport is divided in two layers in the ISZ sediment transport model, an upper and a lower layer. In the lower layer suspended and bed load sediment transport is taken into account. In the upper layer only suspended sediment transport is computed, based on the shear stresses near the bottom.
The sediment concentrations in the upper layer are assumed to decrease, when the water depth increases, resulting in a decreasing sediment transport in the upper layer. Implementation of this assumption by an empirical formula into the model works encouraging well. The model is calibrated against the tests of Koomans in the Scheldt flume (2000).
The model is valid for spilling breaking and the computation area is determined by the non-linearity parameter of the waves, T_{nl}. The non-linearity parameter depends on the wave period and so does the range of the model.

Different field conditions have been investigated in this thesis. Changing transport rates for varying beach slope and sediment composition can be modelled encouragingly well by the developed ISZ sediment transport model. The ISZ sediment transport model requires adjustment when field conditions like wave height and wave period change, since the friction factor and the sediment concentrations change under changing field conditions.
Based on the described changes in sediment transport in literature, under these changing field conditions, a recommendation is made how to adjust the model parameters. The friction, f_w and the bed/suspended load efficiency factors ε_b, ε_s respectively, are used to represent the described changes in sediment transport under these changing field conditions.

Table of contents

1 INTRODUCTION 1

1.1 GOAL 1
1.2 LAYOUT OF THE REPORT 2

2 INNER SURF ZONE MODEL 3

2.1 INNER SURF ZONE MODEL AREA 3
2.2 SETUP OF THE INNER SURF ZONE MODEL 4
2.2.1 Parameterisation of the intra wave layer and flow field 5
2.3 CALIBRATION AND VALIDATION OF THE INNER SURF ZONE MODEL 7
2.3.1 Calibration 8
2.3.2 Validation 10

3 INNER SURF ZONE SEDIMENT TRANSPORT MODEL 11

3.1 ENERGY APPROACH OF BAILARD 11
3.2 INNER SURF ZONE SEDIMENT TRANSPORT MODEL 12
3.2.1 Intra wave sediment transport 12
3.2.2 Sediment transport rates along the beach profile 13
3.2.3 Transport in the upper and lower layer 14
3.2.4 Influence of the decreasing bore height on the sediment transport 15
3.2.5 Friction factor(f_w) in the model 16
3.2.6 Velocities in the model 18

4 SENSITIVITY ANALYSIS 19

4.1 THE INFLUENCE OF THE UPPER AND LOWER LAYER 19
4.2 THE INFLUENCE OF THE FRICTION FACTOR 22
4.2.1 Important factors on the friction factor used here 23
4.3 INFLUENCE OF THE BED LOAD/SUSPENDED LOAD 24
4.4 CONCLUSIONS 26

5 CALIBRATION AND VALIDATION 27

5.1 CALIBRATION TO KOOMANS 27
5.1.1 Calibration parameters 28
5.1.2 Validity 30
5.2 MODEL RESPONSE TO CHANGING FIELD CONDITIONS 31
5.2.1 Wave height 31
5.2.2 Wave period 32
5.2.3 Grain density/size 33
5.2.4 Beach slope 36
5.3 CONCLUSIONS 37

6 CONCLUSIONS AND RECOMMENDATIONS 39

6.1 CONCLUSIONS 39
6.2 RECOMMENDATIONS 40

7 REFERENCES 41

1 Introduction

Beaches and coastal areas are continuously subjected to erosion and accretion. This erosion and accretion strongly depends on the conditions of the sea and the sediment composition in the sea and on the beach. The beach slope always tends to move to a state of equilibrium, implying a zero net sediment transport rate. This equilibrium profile varies due to varying hydraulic conditions, varying from summer to winter, from location to location and from storm to storm.

For many years scientists try to predict these variations in the beach profile. Several models have been developed in recent years to compute the variations in the coastal profile. However, these models fail in a region close to the shoreline, since the parameterized wave models (like Battjes Janssen, 1978) fail in this region. One of the models developed to compute the coastal profiles under varying circumstances is Unibest-TC (Bosboom et al., 1997). This model fails in a region close to the shoreline where the actual wave height exceeds the maximum wave height due to a lack of dissipation mechanisms. Therefore Unibest-TC ceases computations at some distance before the shoreline, at water depth 0.20-0.60[m], depending on the wave period. From this point on Unibest-TC uses a linear extrapolation to zero of the sediment transport rate in the last computed cell up to the final cell.

In this thesis a model has been developed to compute the sediment transport rates up to zero meter water depth. The model is based on the hydrodynamic inner surf zone model of Aarninkhof (1999) and uses the energy based sediment transport mechanism of Bailard (1981). The inner surf zone model is founded on the self-similarity of bores propagating onshore through the inner region, observed by Svendsen et al. (1978). The inner region, discussed in paragraph 2.2, originates from Svendsen et al (1978). The inner surf zone sediment transport model aims to simulate the sediment transport through the inner region up to zero meter water depth.

1.1 Goal

The sediment transport rates in the inner surf zone up to zero meter water depth are estimated by extrapolation from the point where Unibest TC ceases computations. A computation model for sediment transport rates would increase the understanding and accuracy of the transport rates in the inner region.

The objective of this thesis is:

To simulate the sediment transport processes of this inner surf-zone, the parameters and their influence on the sediment transport.

This leads to the following sub-objectives:

1. Develop a sediment transport model valid for the inner surf zone, which can predict sediment transport rates through the inner region up to zero meter waterdepth.
2. Investigation of the influences of the different model parameters (friction, bed/suspended load efficiency and layer contribution) and test the sediment transport models' sensitivity to these parameters.

3. Illustrate and describe the effect of changing the conditions on the sediment transport rate (Beach slope, beach material, wave height, etc.)

1.2 Layout of the report

The report starts with a description of the hydrodynamic inner surf zone model of Aarninkhof, (2001) on which the inner surf zone sediment transport model is founded. The inner surf zone model computes the wave set up and wave height in the inner surf zone and the velocities through the inner surf zone.
The next part, chapter 3 starts with a description of the sediment transport formula of Bailard, used in the inner surf zone sediment transport model. Further the set up of the model is reviewed. The background and the implementation of the friction factor (f_w), velocity (v) and shear stress (τ) in the model is described.

In the following chapter 4 the inner surf zone sediment transport model is subject to a sensitivity analysis. The important model parameters are varied (friction, layer influence and efficiency coefficients for the suspended and bed load ε_s, ε_b respectively) and the influences on the sediment transport rates due to changing these parameters are illustrated and discussed..

In chapter 5 the model is calibrated against the data of Koomans (2000) by setting the model parameters, friction and layer contribution coefficients. The influence of the conditional parameters (wave period, wave height , grain density, grain size and beach angle is illustrated and reviewed. The computed sediment transport in the ISZ sediment model for the changing conditions is compared to the field observations described in literature. Based on what found in the literature a recommendation is made how to vary the model parameters, bed/suspended load efficiency and friction, f_w to represent what was found in literature over the changing field conditions.

Finally the conclusions are drawn and recommendations are given for further investigation.

2 Inner surf zone model

The hydrodynamics of the inner surf zone or 'inner region' Svendsen (1978) are modelled in the inner surf zone model, Aarninkhof (1999).
The inner surf zone model (ISZ-model) of Aarninkhof (1999) is discussed and will form the base for the inner surf zone sediment transport model. The ISZ model determines the hydrodynamics up to zero water depth, trough the 'inner region' Svendsen (1978) for spilling breakers.
After reviewing the area modelled in the ISZ model, the set up of the model is discussed. The calibration to the tests of Stive (1980) and the validation of the model based on Irribarren's breaking parameter are discussed in the last paragraph.

2.1 Inner surf zone model area

The time averaged water level through the surf zone increases induced by the loss of wave momentum. Spectral models (e.g. Battjes and Janssen (1978); Thornton and Guza (1983)) describe the wave transformations across the surf zone relatively well. However, they predict the steepest rise of the water level too far seaward (Battjes and Stive (1985)). These models have been extended with the roller formulation**,** Svendsen (1984), modified according to Stive and De Vriend (1994). This causes a delay of the dissipation of turbulent kinetic energy, resulting in a shoreward shift of the steepest water level rise.
However the models fail in the region close to the shoreline, where the actual, wave height H_{sig} exceeds the maximum wave height H_{max}, due to a lack of dissipation meganisms, Battjes and Janssen (1978).

An operational model like Unibest-TC deals with this by ceasing computations at some distance of the shoreline, with the help of a dimensionless parameter T_{nl} representing the non-linearity of the wave field:

$$T_{nl} = T_{peak}\sqrt{\frac{g}{h}} \qquad \textit{Equation 2-1}$$

In which:

- T_{peak} *is the peak period of the waves* *[s]*
- *G is the gravitational constant* *[m/s^s]*
- *H is the local water depth* *[m]*

The default value of T_{nl} is set to 40 *[-]*, which causes the model to terminate computations at water depths of 0.2-0.6 *[m]* for wave periods T_{peak} ranging from 5 to 10 *[s]*. From this point Unibest-TC uses a linear extrapolation of the transport to last grid cell.

2.2 Setup of the inner surf zone model

To determine inner surf zone hydrodynamics up to zero water depth the inner surf zone model was developed Aarninkhof (1999). The term inner surf zone comes from the inner region originating from Svendsen et al.(1978). See figure (2-1).

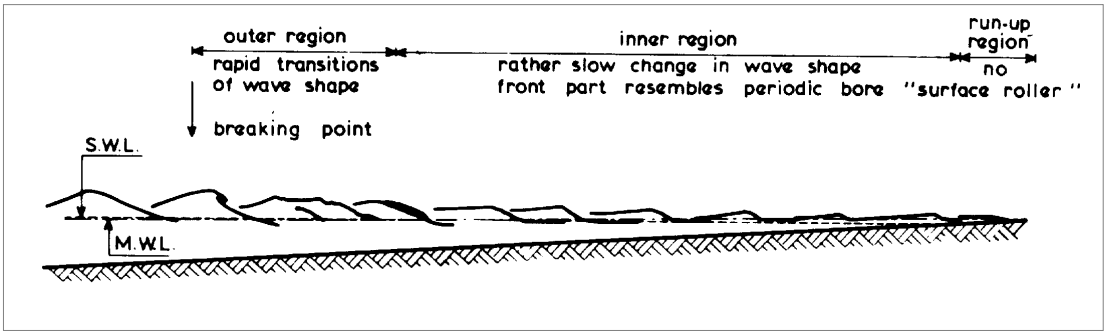

Figure 2-1, *Wave characteristics in the inner surf zone according to Svendsen et al.(1978).*

The inner surf zone model is based on the self-similarity of the bores propagating onshore through the inner surf zone. In the outer region chaotic breaking takes place, in the inner region or inner surf zone a relatively well-organised motion is developed quickly. The breaking motion is fully turbulent, while the mean motion is quasi steady. Until the shoreline is reached the quasi steady (or bore motion) is maintained.
The self-similarity of the bores in the inner region was observed by Svendsen et al. (1978) and is confirmed by the flume experiments of Stive (1980).
The wave shapes propagating trough the inner surf zone are highly similar. This conservation of wave shape even holds for waves at the same position, originating from different deep water conditions. From the nearly constant ratio of wave height over mean water depth it can be concluded that the water motion at each point in the inner surf zone is strongly locally controlled. This constant ratio is used to determine the extend of the inner region.

The inner surf zone model simulates the type of bores described here and uses a two layer approach see figure 2-2. In the upper layer a bore height H_2 propagates onshore with velocity V over a bed with slope m. The onshore mass flux initiated in the upper layer is compensated by a net offshore mass flux in the lower layer, with height H_1. The H_{mean} is the water depth, averaged over the wave period.

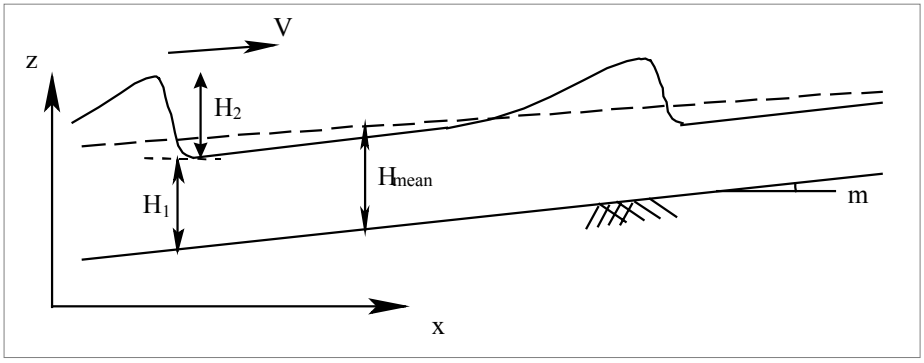

Figure 2-2, *Schematic review of the layers.*

To predict the bore height decay and the associated set-up through the inner surf zone, a time averaged mass and momentum conservation has been developed. In order to do so intra-wave expressions for the bore height and flow field in the layers are needed.

The intra wave time scale ranges from [0,T]. These intra wave expressions can be integrated over the wave period to get time averaged model variables. The intra wave expressions have been parameterised and are reviewed here.

2.2.1 Parameterisation of the intra wave layer and flow field

The flume measurements by Stive (1980) and the conceptual model of a quasi steady breaking wave after Peregrine and Svendsen (1978) are used for parameterisation of intra-wave surface elevation and flow fields as a function of the intra wave time, t*= t/T *[-]*. These test results have been used in a depth-averaged sense, to arrive at the parameterisations shown in figure 2-3.

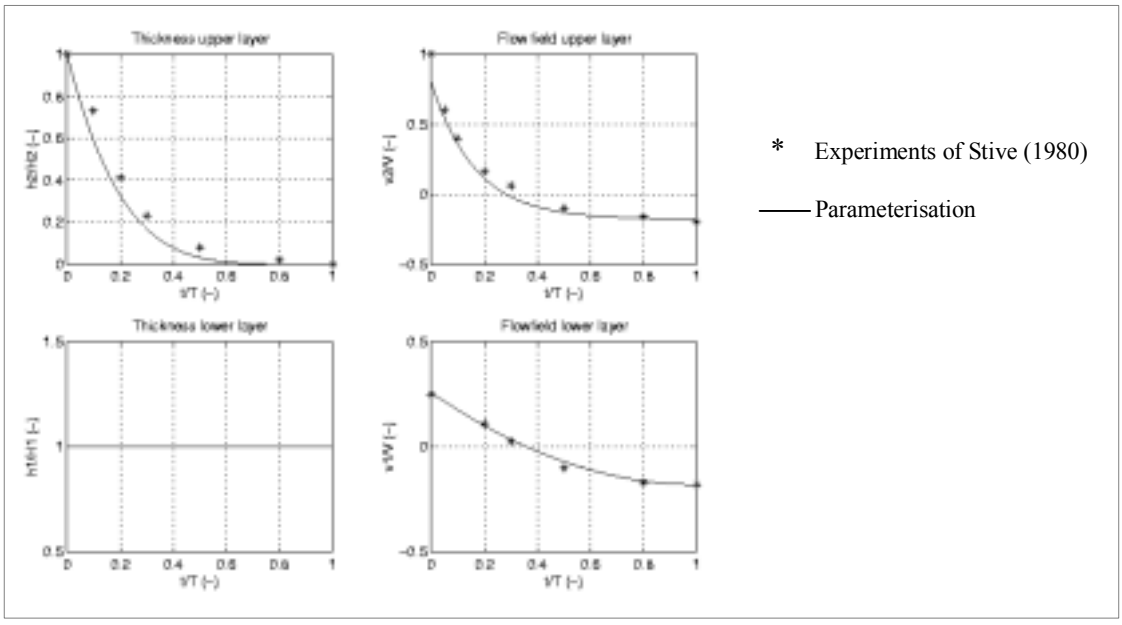

Figure 2-3, *Parameter of intra-wave layer thickness and flow field.*

The upper layer has an intra wave height h_2 and an intra wave propagation speed v_2. The intra wave thickness of the lower layer is constant $(h_1/H_1)=1$ *[-]*.
On t*= 0 *[-]* the bore passes and the velocity v_2/V_2 *[-]*, as well as the layer thickness h_2/H_2 *[-]* are on their maximum, after the passing of the bore those values rapidly decrease.
The onshore mass flux trough the upper layer is compensated by a net offshore mass flux in the lower layer with depth H_1 and velocity distribution v_1/V_1. The velocity in the lower layer decreases slowly and becomes negative, due to the seaward directed return flow.

The solid lines in figure 2-3 represent the parameterisations. The equations (2-2 to 2-5) for these lines read:

$$\frac{h_1}{H_1} = 1$$ ***Equation 2-2***

$$\frac{h_2}{H_2} = (1 - \frac{t}{T})^a$$ with a = 5 ***Equation 2-3***

$$\frac{v_1}{V} = b(1 - \frac{t}{T})^2 + c$$ with b = 0.44 and c = -0.18 ***Equation 2-4***

$$\frac{v_2}{V} = p \cdot e^{q(1-\frac{t}{T})} + s$$ with p= 0.0024, q = 6 and s=-0.18 ***Equation 2-5***

In which:

- h_1: *intra wave thickness of the lower layer* *[m]*
- h_2: *intra wave thickness of the upper layer* *[m]*
- H_1: *thickness of the lower layer* *[m]*
- H_2: *boreheight at the borecrest* *[m]*
- v_1: *flow velocity of the lower layer* *[m/s]*
- v_2: *flow velocity of the upper layer* *[m/s]*
- V: *bore propagation speed* *[m/s]*

Once the flow velocities in the lower and upper layer have been parameterised as a function of the bore propagation speed V, the inner surf zone model can be formulated in three variables:

1. *Lower layer thickness, H_1*
2. *Upper layer thickness, H_2*
3. *Bore propagation speed, V*

The integration of the intra-wave equations 2-2 to 2-5 over time yields the time-averaged fluxes of mass and momentum in both the upper and the lower layer. The condition for mass and momentum balance in the inner surf zone provides two equations 2-7 and 2-8 respectively. The system of equations is completed with the shallow water wave propagation equation, 2-6.

Shallow water approximation for bore propagation

$$V = \sqrt{g(H_1 + \delta \cdot H_2)}$$ ***Equation 2-6***

In which:

- g: *gravitational acceleration* *[m/s^2]*
- δ: *'uncertainty' coefficient* *[-]*

The δ is in order of 0.5-1 *[-]*. The coefficient accounts for the uncertainty in the absolute magnitude of V.

The mass balance (2-7) implies that the net shoreward mass flux in the upper layer is compensated by the net seaward mass flux through the lower layer.

$$M_{onshore} = M_{offshore} \Leftrightarrow \int_0^1 \int_0^{h_2} (\rho v_2)\, dz dt_* = \int_0^1 \int_0^{h_1} (\rho v_1)\, dz dt_* \qquad \textit{Equation 2-7}$$

In which:

- ρ: *water density* *[kg/m3]*
  (Constant value, aeration is not taken into account)
- t^*: *dimensionless intra wave time t/T* *[-]*

The mass balance is solved numerically after substitution of the parametric formulations (equation 2-2 to 2-5).

In the time averaged momentum balance the entire two-layer system is taken into account. The conservation of horizontal momentum with a cross-shore reference volume is taken in a "closed" area, bordered by the bottom, water surface and vertical planes.
The momentum balance reads:

Equation 2-8

$$\underbrace{\frac{d}{dx}\int_0^1 \int_0^{h_2} p\, dz dt_*}_{\text{(I)}} + \underbrace{\frac{d}{dx}\int_0^1 \int_0^{h_2} (\rho v_2^2)\, dz dt_*}_{\text{(II)}} + \underbrace{\frac{d}{dx}\int_0^1 \int_0^{h_1} (\rho v_1^2)\, dz dt_*}_{\text{(III)}} + \underbrace{\frac{d}{dx}\int_0^1 \int_0^{h_1+h_2} p_0 dz dt_*}_{\text{(IV)}} + \underbrace{\int_0^1 p_b \frac{dz_b}{dx} dt_*}_{\text{(V)}} + \underbrace{\int_0^1 \tau_b dt_*}_{\text{(VI)}} = 0$$

In which:

- τ_b: *bottom shear stress* *[kgm^2/s^2*m^3]*

The first term represents the net contribution of the momentary horizontal pressure distribution across the upper layer. This pressure is assumed to be hydrostatic. The second and third term represent the horizontal momentum fluxes through the upper and lower layer. The fourth term adds the net effect of hydrostatic pressure caused by the sloping mean water level. The fifth term is for horizontal force induced by the sloping bottom. The last term represents the contribution of the bottom friction.

2.3 Calibration and validation of the inner surf zone model

The previous two paragraphs showed the inner region Svendsen et al. (1978), characterised by the self-similarity of the bores. The ISZ-model is based on this self similarity of bore propagation through the inner region. The parameterisations in combination with the shallow water approximation for bore propagation, the mass balance and momentum balance enables it to compute the bore propagation speed (V), lower layer thickness (H_1) and upper layer thickness (H_2).
In this paragraph the ISZ-model's calibration and the validation, depending on the breaker type is discussed.

The inner surf zone model has been compared to the flume experiments by Stive (1980). The experiments were restricted to two wave conditions, test 1 and test 2. Both tests refer to spilling breaking (see paragraph 2.3.2).

The inner surf zone model has been applied to predict the bore height decay and wave set up through the inner region of the tests done by Stive (1980).
The measured wave height and water depth at the seaward end of the inner region are the boundary conditions for the inner surf zone model here. The upper layer is related to the water motion above through level (H_2=H_{meas}). To make sure the time-averaged elevation of the surface is continuous across the seaward boundary of the model the thickness H_1 of the lower layer should obey the relationship

$$z_{surf,meas} = z_{surf,bc} \Leftrightarrow z_{swl} + \eta = z_b + H_1 + \int_0^1 h_2 dt_* \qquad \textit{Equation 2-9}$$

In which:

- z_{swl}: *still water level* *[m]*
- η: *measured wave set up* *[m]*
- z_b: *bottom elevation (at the boundary location)* *[m]*

2.3.1 Calibration

Two tuning parameters are used for the calibration, the friction factor f_w and the lower layer flow control parameter.

Aarninkhof (1999) introduced a tuning parameter, which affects the parameterisation (equation 2-3) of the lower layer according to:

$$\frac{v_1}{V} = \left(1 + \frac{\mu}{2}\right) \cdot a \cdot \left(1 - \frac{t}{T}\right)^2 + (1 - \mu) \cdot c \qquad \textit{Equation 2-10}$$

A positive μ increases the onshore velocities in the lower layer during the passing of the bore and decreases the velocities in the wake region that follows. So a positive μ decreases the net offshore flow in the lower layer. Negative values for μ do the opposite.

In figure 2-4 the sensitivity of the lower layer flow field to variations of μ over a realistic calibration range from – 0.10 to 0.10 *[-]* is given. As can be seen the modified flow field still fits the measurements reasonably well and does not violate the starting point of self-similarity of the water motion in the inner region.

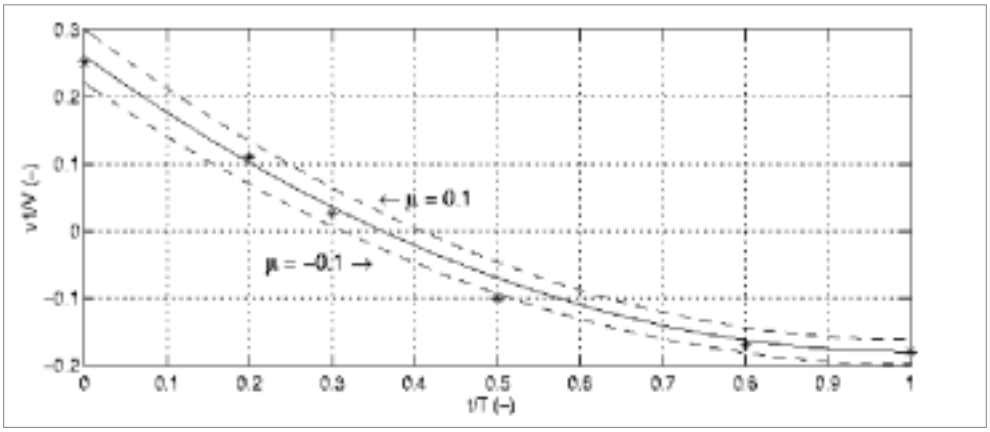

Figure 2-4, *Sensitivity of flow field lower layer to tuning parameter μ..*

The friction factor, f_w is the second factor used to calibrate the inner surf zone model.
In equation 2-8,(VI) the friction factor can be found in the shear stress.

$$\tau_b = 0.5 f_w \cdot v_l^2 \qquad \textit{Equation 2-9}$$

To the calibration of the model against the test of Stive(1980), the following values are used:

Table 2-1 *Calibration values against Stive, 1980*

Parameter	Friction, f_w	μ
Test 1	0.10	0.04
Test 2	0.25	0.10

The calibration is plotted in figure 2-5.

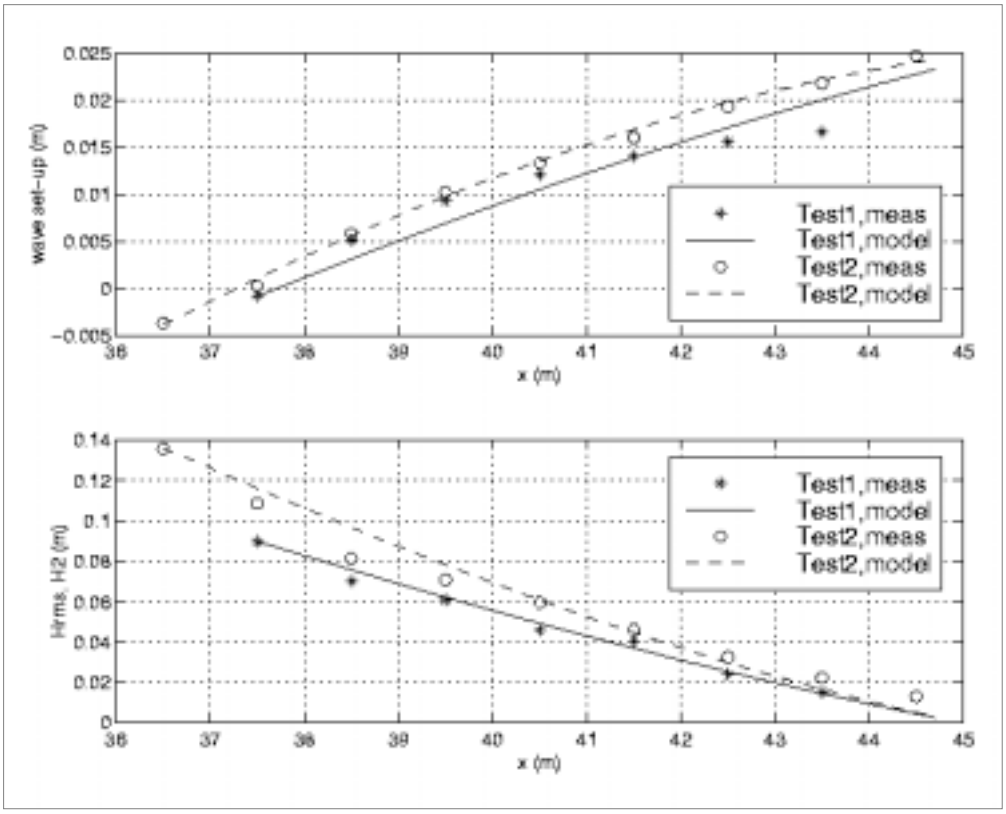

Figure 2-5, *Model predictions of bore height and wave set-up versus measurements of Stive (1980)*

Both tests perform well with relative large friction numbers, which indicates high shear stresses in the inner region, due to high turbulence.
The setting of the tuning parameter μ fits well within the margins of uncertainty (see figure 2-4), with regard to the magnitude and shape of the velocity field in the lower layer.

2.3.2 Validation

Since the model has only been tested against the tests of Stive (1980) under spilling breaker types, the model's validity is supposed to be only within the range of this breaker type.

Waves break in a different way depending on the beach slope and the wave steepness. Three main types of breaking can be classified: surging, plunging and spilling breakers. The transition from surging to plunging is often referred to as collapsing breaking.

Irribarren, (1938) introduced a parameter for the classification of the breaker types (for classification of the breaker types, see figure2-6). This parameter separates the different breaker types.

$$\xi = \frac{\tan\alpha}{\left(H_s / L_0\right)^{1/2}} \qquad \textit{Equation 2-20}$$

In which:

- H_s *is local wave height [m]*
- L_0 *deep water wave length [m]*
- ξ *Irribarren's dimensionless parameter*
- $tan(\alpha)$ *slope [-]*

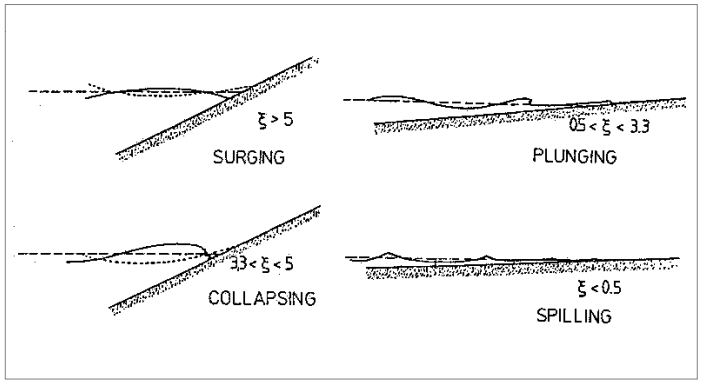

***Figure 2-6**, Breaker types according to Irribarren*

To determine the validity range of the inner surf zone model the breaking range of the test by Stive(1980) is used. The wave conditions of the test by Stive are summarised here and the breaking types are calculated from the measurements.

***Table 2-2,** Test parameter values and their breaking parameters*

Parameter	H_0	$T_{wave\ maker}$	$H_{breaker}$	H_0/L_0	Irribarren, ζ	Breaker type
Test 1	0.159	1.79	0.178	0.032	0.140	Spilling
Test 2	0.142	3.00	0.226	0.010	0.257	Spilling

So according to Irribarren's parameter, the tests of Stive (1980) are in the range of the spilling breaking. The validity of the model is supposed to be in the range of the tests, to which the model is calibrated, the spilling breaker area. Spilling breaking can be found on gentle sloping beaches.

The ISZ model Aarninkhof (1999) forms the base of the ISZ sediment transport model, discussed in the next chapter. The ISZ sediment transport model computes the sediment transport rates along the beach profile, through the inner region.

3 Inner surf zone sediment transport model

A new sediment transport model for the inner surf zone is presented based on the inner surf zone model of Aarninkhof (1999). The sediment transport computations in the ISZ-sediment transport model are based on the energy based transport mechanism of Bailard (1981). After a short review of this energy approach an implementation is given for this approach in the ISZ sediment transport model.
Furthermore, the water layer separation used in the ISZ sediment transport model, the friction factor (f_w) used to determine the work done by the fluid and the water velocities, used in the ISZ sediment transport model, are discussed.

3.1 Energy approach of Bailard

Bagnold (1963;1966) introduced the idea that sediment transport is related to energy dissipation. This approach assumes that a part of the energy is used to move the sediment grains or keep the sediment in suspension.
Bailard (1981) used Bagnold's total load transport for streams to develop a total load model of time varying sediment transport over a plane sloping bed. The sediment transport rate is assumed to be directly related to the energy dissipation rate. This dissipated energy (fluid power) is equal to the work done by the fluid.

Fluid power:

$$P(t) = \tau \cdot u_t \qquad \textit{Equation 3-1}$$

In which:

- τ: *shear stress* *[N/m^2]*
- u_t: *fluid velocity* *[m/s]*

The expression for the sediment transport rate is:

$$q(t) = [K_b(t) + K_s(t)] \cdot \frac{P(t)}{(\rho_s - \rho)g} \qquad \textit{Equation 3-2}$$

K_b and K_s are dimensionless time varying factors, which represent the bedload and suspended load in the expression for the sediment transport respectively. K_b and K_s can be determined by equations 3-3 and 3-4 respectively.

$$K_b(t) = \frac{\varepsilon_b}{\tan\phi} \cdot \left(\frac{u(t)}{|u(t)|} - \frac{\tan\beta}{\tan\phi} \right)$$ **Equation 3-3**

$$K_s(t) = \frac{|u(t)|}{w_s} \cdot \left(\frac{u(t)}{|u(t)|} - \varepsilon_s \tan\beta \frac{|u(t)|}{w_s} \right)$$ **Equation 3-4**

In which:

- w_s : *fall velocity of a grain* *[m/s]*
- ϕ: *angle of internal stability of the sediment* *[^{o}]*
- β : *beach slope angle* *[^{o}]*
- *Bagnold introduced a factor ε_s for the suspended load, assuming that the power consumed to transport the suspended load is a constant fraction of the total power produced by the stream. Bailard found 0.025 for the value of ε_s.*
- *ε_b is the bed load efficiency factor (0.21)*

3.2 Inner surf zone sediment transport model

The ISZ sediment transport model will be reviewed here. The model is based on the ISZ model by Aarninkhof (1999) as described in chapter 2. The ISZ sediment transport model imports the bore propagation speed (V) signal and the boreheight at the borecrest (H_2) signal from the inner-surf zone model. The energy approach of Bailard is used to describe the sediment transport processes.

The ISZ sediment transport model starts with computing the intra-wave sediment transport rates (intra wave time is defined as t/T, ranging from [0,T]) through the inner region. The inner region, from the starting point of computations to zero meter water depth, a number of points (X_1, …, X_i) are observed. The number of these inner region points depends on the grid size and the computation area of the model. Integration of the sediment transport rates over the wave period for these points yields a net sediment transport rate for each point. Plotting all these points and their net sediment transport rate results in a net sediment transport graph along the beach profile, see figure (3-2)

3.2.1 Intra wave sediment transport

The sediment transport model uses the energy dissipation rate of the fluid to determine the sediment transport rate according to Bailard (1981). This dissipated energy or fluid power is computed according to equation 3-1. The input for this equation is the shear stress, τ and the fluid velocity u(t). The fluid velocity u(t) can be computed by using the intra wave equations after importing the bore propagation speed (V) from the inner surf zone model.
To determine the shear stress the fiction factor, f_w is needed. The shear stress is formulated as:

$$\tau = f_w . \rho . u_t^2$$ **Equation 3-5**

In which

- f_w : *dimensionless friction factor* *[-]*

The value of the dimensionless friction factor ranges from 0.005 *[-]* to 0.03 *[-]* and will be discussed in paragraph 3.4.
The dimensionless sediment transport parameters K_b and K_s for bed load and suspended load sediment respectively can be computed according to equations 3-3 and 3-4. The velocities used in equations 3-3 and 3-4 refer to the fluid velocities u(t) and can be computed by using the intra wave equations (2-2, 2-5) after importing the bore propagation speed (V) from the inner surf zone model.
The sediment transport rate, q(t) *[$m^3/(m*s)$]* can now be determined according to equation 3-2. This yields an intra wave sediment transport rate over the wave period on time scale t/T*[-]* for the chosen cross-shore location in the inner region.

In figure 3-1, the intra wave sediment transport rate, computed by the ISZ sediment transport model is printed. The location of the plot represents a location in the inner region with water depth h = 0.20 *[m]* on a beach where spilling breaking occurs under the conditions listed below.

The settings:

- *Water depth h= 0.20* *[m]* *(depth on chosen cross shore location)*
- *Beach slope, tan β =0.025* *[-]* *(slope 1:40)*
- *Wave height in deep water, H_{rms}= 0.8* *[m]*
- *Wave period, T = 8* *[s]*

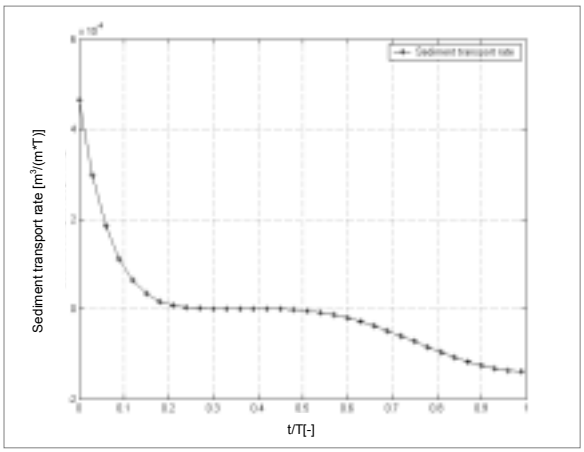

***Figure 3-1**, Intra wave sediment transport rates, for water depth h=0.2[m]*

The intra wave sediment transport shows a large shoreward peak in the sediment transport rate in the first part, this is when the bore passes. In the middle region hardly any activity is shown, in the last part when the velocities in the return flow increase the sediment transport rates become seaward.

3.2.2 Sediment transport rates along the beach profile

Once the sediment transport model has computed the intra-wave sediment transport rates for all computational points in the inner region, (X_1, X_2,…X_i), starting at X_1 (were Unibest-TC ceases computations, depending on T_{nl}) and finishing at X_i (zero water depth), the net sediment transport rate along the beach profile are computed. Integration over the wave period of the intra wave sediment transport rates on all locations (X_1, X_2,…X_i) by equation 3-6 results in a net sediment transport rate along the beach profile.

$$Q_i = \frac{1}{T}\int_0^T q_i(t)dt \qquad \textit{Equation 3-6}$$

Figure 3-2 shows a plot of the net sediment transport, (Q) *[m^3/(m*s)]* against the water depth along the beach profile, through the inner region computed by the ISZ sediment transport model. The conditions are according to the conditions in paragraph 3.2.1. In figure 3-2 the location for the plotted the intra wave sediment transport on waterdepth 0.2*[m]* in figure 3-1 is marked.

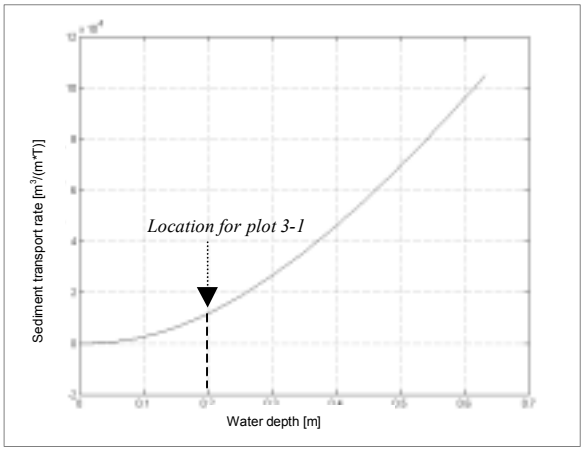

***Figure 3-2**, Net sediment transport rates along the beach profile.*

The net sediment transport rate plot along the beach profile shows a decreasing onshore sediment transport for decreasing water depth and the transport stops when the water depth becomes zero, this implies that the beach is accreting. The ISZ sediment transport model starts its computations here at water depth 0.65 *[m]*, depending on the wave period represented in the non linearity parameter T_{nl} *[-]*, discussed in paragraph 2.1. In figure 3-3 a schematic review is given were Unibest TC ceases computations and the ISZ sediment transport model takes over.

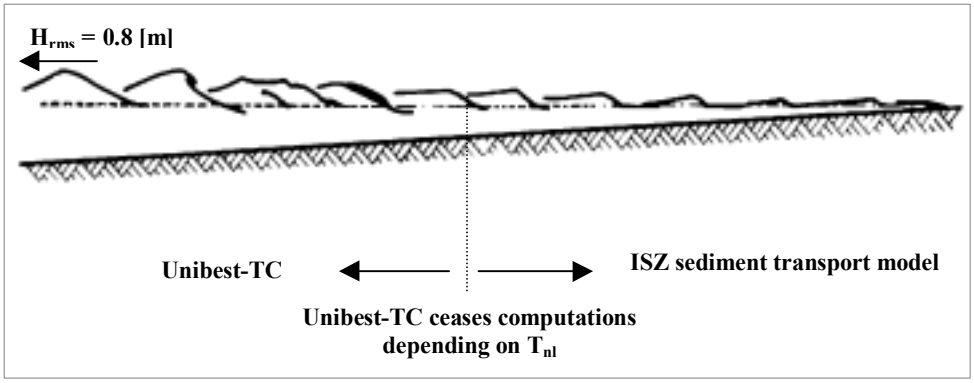

***Figure 3-3**, schematic review of the starting point of the ISZ sediment transport model*

In chapter 5 the net sediment transport rates will be calibrated against the data of Koomans(2000).

3.2.3 Transport in the upper and lower layer

In paragraph 3.2.1 the computation of the intra wave sediment transport rate is discussed. To compute the intra wave sediment transport rates a separation in the sediment transport is introduced, representing the different sediment concentrations in these layers. The water layer separation of the ISZ model, Aarninkhof (2001) is used to make this separation. The sediment

transport is split up in a upper and a lower transport layer, with layer contribution coefficients, C_u and C_l respectively.
In the lower layer it is assumed that both suspended and bed load sediment transport will occur, expressed by the dimensionless transport rate parameters $C_l \cdot K_s$ and K_b respectively, see equations 3-3 and 3-4. In the upper layer only suspended sediment transport expressed by $C_u \cdot K_s$ is assumed to take place.
In figure 3-4 a schematic review is given of the sediment transport layers and their contribution coefficients.

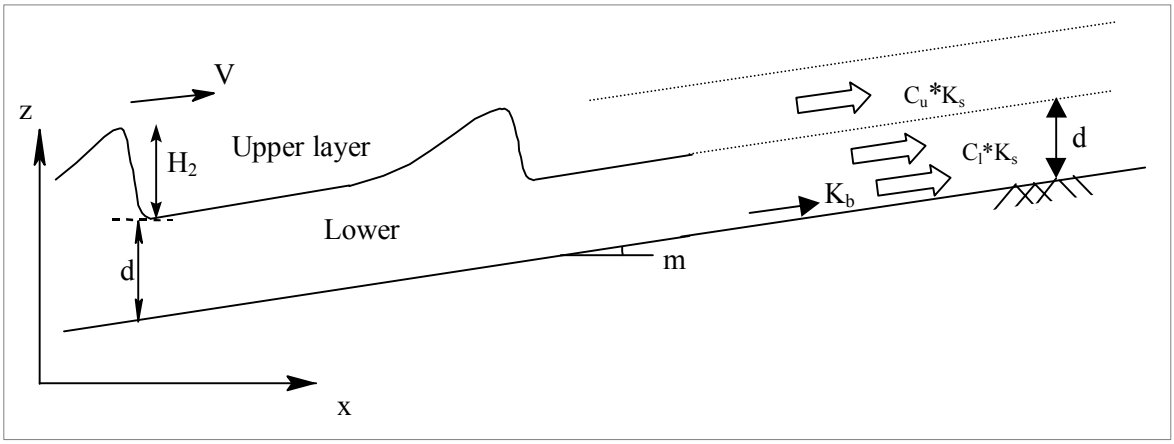

***Figure 3-4**, The layer separation in the inner surf zone sediment transport model*

The dimensionless transport parameter for suspended sediment K_s is separated by a dimensionless suspended transport contribution parameter C_l for the lower layer and C_u for the upper layer.
The K_s is calculated using the velocity in the lower layer. In paragraph (3.5) the velocities used will be further discussed.

The circumstances in the layers differ from each other: different heights, different suspended sediment concentrations and therefore their contribution to the suspended sediment transport rate is assumed to be different too. To take these different contributions into account, dimensionless sediment transport contribution coefficients are introduced, C_l and C_u for the lower and upper layer respectively. Attention must be paid that the sum of these sediment transport contribution coefficients for the suspended load, in the lower layer C_l and upper layer C_u equals 1, see equation 3-7.

$$K_s = C_l \cdot Ks + C_u \cdot Ks \qquad \textit{Equation 3-7}$$

In paragraph (4.1), the influence of these layer contribution coefficients is investigated. The contribution coefficients will vary from (0.8-1) for the lower layer (C_l) and from (0-0.2) for the upper layer (C_u).

3.2.4 Influence of the decreasing bore height on the sediment transport

To compute the suspended sediment transport rate, Bailard (1981) used the averaged waterdepth.
In figure 3-5 it can be seen that the thickness of the upper layer rapidly decreases after the passing of the bore. Since the thickness of the upper layer decreases, the sediment transport will also decrease, directly related to the layer thickness.

The decrease of layer thickness must be taken into account in the Bailards approach, since the average water depth is used by Bailard (1981).
To do so, a dimensionless parameter (equation 3-8) is introduced. This parameter represents the influence of the decrease of the upper layer thickness on the sediment transport.
The dimensionless transport correction parameter has the shape:

$$h_2/H_2\ [-] \qquad \textit{Equation 3-8}$$

In which:
h_2: *Time dependant boreheight* *[m]*
H_2: *Maximum boreheight* *[m]*

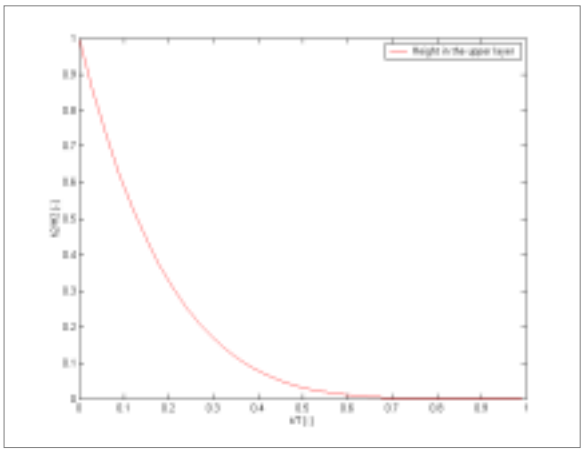

Figure 3-5, *The relative bore height on an intra wave time scale*

The sediment transport correction parameter decreases the suspended sediment transport rate, representing the decrease of the upper layer thickness. The contribution of the upper layer to the sediment transport becomes zero when the layer thickness in the upper layer decreases to zero.

3.2.5 Friction factor(f_w) in the model

To determine the shear stress, τ (equation 3-5) the friction factor, f_w is needed. Several approaches have been developed to determine the correct value of the friction factor. The approach of Bagnold will be discussed here.
However the friction factor can also be obtained from conducted field data, as described by Puleo and Holland (2001).
The field data describes a range for the value of the friction factor varying from 0.01 to 0.03, while the approach of Bagnold yields a constant value for the friction factor.
In Chapter 4, the influence of varying the friction factor, f_w over the range described by Puleo and Holland(2001), on the sediment transport rates will be discussed and illustrated.

Friction factor according to Bagnold

Bagnold uses the shear velocity to determine the work done by the fluid.
He introduced the following expression for a rough turbulent flow:

$$\frac{u}{u_*} = \frac{1}{\kappa}\ln\frac{y}{ks} + 8.50 \qquad \textit{Equation 3-9}$$

In which:

- u_*: *shear velocity* *[m/s]*
- u: *water velocity* *[m/s]*
- y: *grain level* *[m]*
- k_s,: *Nikuradse roughness length* *[m]*
- κ,: *Von Karman's constant, 0.4* *[-]*

Assuming the presence of a rough bed Bailard introduces $y = k_s$.
Doing so expression 3-8 becomes:

$$u = \frac{u_*}{8.5}$$ ***Equation 3-10***

When using the shear velocity to determine the shear stress the expression for the shear stress becomes:

$$\tau = \rho \cdot u_*^2$$ ***Equation 3-11***

In which:

- τ : *shear stress* *[kgm^2/s^2*m^3]*
- ρ : *water density* *[kg/m^3]*
- u_*: *is the shear velocity* *[m/s]*

Inserting equation (3-9 in 3-10) yields:

$$\tau = \rho \cdot \left(\frac{u}{8.5}\right)^2$$ ***Equation 3-12***

Comparing equation 3-11 with equation (3-5) the value for the friction factor can be obtained. The friction factor according to Bailard becomes $(1/8.5)^2$, $f_w = 0.0138$ *[-]*.
This value is constant over the tidal cycle.

Friction factors from the field

Puleo and Holland (2001) have performed field measurements and observations and came up with an empirical value for the swash zone friction coefficient. According to their findings this value changes in time. The friction factor changes trough the tidal cycle and is different for uprush and backwash. The field investigation, by Puleo and Holland (1994, 1997), resulted in a friction factor for the uprush that is constant over the swash cycle set between 0.005 to 0.01*[-]*. The backwash friction coefficient however was found to be bigger than the uprush friction factor. It was also found that the backwash friction coefficient changes during the tidal cycle. The backwash friction values range from 0.01-0.03 *[-]* changing through the tidal cycle.

Table 3-1, *Range of friction factor values according to Puleo and Holland*

Tide cycle	*Uprush*	*Backwash*
High	0.05-0.01	0.01
Low	0.05-0.01	0.03

According to what was found by Puleo and Holland (2001) the friction factor's value, f_w is constant for the uprush over the swash cycle. This implies that the net transport rate depends on the fluctuations of f_w over the tidal circle in the backwash.

3.2.6 Velocities in the model

Bailard's sediment transport approach (1981) is based on the two-dimensional stream flow model of Bagnold (1963;1966) which uses the depth integrated average velocity of the stream, u_m in his model.

$$u_m = \frac{1}{h}\int_0^h u \cdot dz \qquad \textit{Equation 3-13}$$

The method of Bailard (1981) is developed for a time varying flow and therefore uses the time varying average water velocity u(t), to compute the shear stress (τ) and dimensionless transport rate coefficients, K_s and K_u.

The ISZ model computes the maximum velocity V for a passing wave on t/T = 0. Using the intra-wave equations 2-2 to 2-5, the time dependent velocities in the upper, v_u and lower layer v_l can be computed.
The average velocity in the lower layer v_l , assumed to be constant over the depth of the layer is used in the ISZ sediment transport model to determine the:

- Shear stress(τ), equation 3-5.
- Dimensionless bed load sediment transport factor(K_b), equation 3-3.
- Dimensionless suspended sediment transport factor (K_s), equation 3-4.

4 Sensitivity analysis

In chapter 3 the ISZ-sediment transport model's separation of the water layer into a upper and a lower layer was already mentioned. Together with the friction factor f_w and the bed load efficiency factor, ε_b they form the most important influencing parameters on the sediment transport rates.
The layer separation is used to separate the sediment transport processes in the upper and lower layer. Layer contribution coefficients, C_u and C_l for the upper and lower layers respectively are introduced, representing the different sediment concentrations in the layers. The layer contribution coefficients will be varied and the influences of this variation on the sediment transport rates will be discussed.
The friction factor, f_w (used to determine the fluid power) will be varied over the range described by Puleo and Holland (2001) and the influences will be illustrated and reviewed. The bed load efficiency factor is varied over the range described by Bailard (1981). The suspended load efficiency factor ε_s does not show significant influence on the sediment transport rates within it's range described by Bailard (1981).
During these variations the setting of Koomans simulations in the Scheldt flume (2000) are used.

- *Beach slope plane, tan β:* *0.025* *[-]* *(slope 1:40)*
- *Wave height, H_{mo}:* *0.17* *[m]*
- *Wave period, T_p:* *2* *[s]*
- *Fall velocity, w_s:* *0.012* *[m/s]*
- *Grain diameter, d_{50}:* *129* *[μm]*
- *Grain diameter, d_{90}:* *187* *[μm]*

4.1 The influence of the upper and lower layer

The separation of the water layer in a upper and a lower layer, resulting in a separation of the sediment transport contribution was already mentioned. The influence of this layer separation on the sediment transport rate will be reviewed.

The energy based sediment transport approach of Bailard (1981), used in the ISZ sediment transport model, uses a constant value for the sediment concentration over the water depth. According to Van der Velden (1989) the sediment concentration however has a logarithmic distribution over the water depth, see figure 4-1.

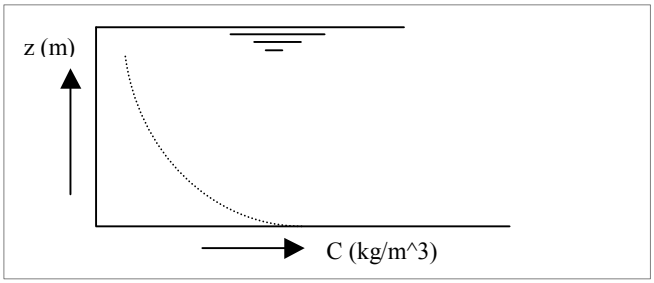

Figure 4-1, *Sediment concentration profile over the water depth.*

The ISZ sediment transport model applies concentration coefficients C_u and C_l for the upper and lower layer respectively, to account for the type of sediment concentration as described by Van der Velden (1989).

The contribution coefficients C_u and C_l are dependent on each other, since the sum of the coefficients has to be 1. The lower layer contribution coefficient is varied in a range from 0.8 to1 and the upper layer coefficient from 0.2 to 0. The influences on the intra wave sediment transport rates of these layer contribution coefficients are illustrated in plots (4-2a) and (4-2b). In figure (4-3) the influence on net sediment transport rate along the beach profile of varying the layer contribution coefficients is illustrated. The range of the layer contribution coefficients and their line types in the plots are listed in table 4-2.
The range of the layer contribution coefficients is an estimation, based on the wave height and sediment concentration profile along the water depth (see figure 4-1). The ratio between upper and lower layer of $C_l = 0.1$ and $C_u = 0.9$ is considered to be the most likely value.
Simulation no.1 refers to the sediment transport situation described by Bailard (1981), a situation with no layer separation. Simulations 2 and 3 refer to the sediment transport situation with the layer separation as described above.

Table 4-1, *Values for the layer contribution*

Simulation	C_l	C_u	Line type
1	1.0	0	*
2	0.9	0.1	-
3	0.8	0.2	o

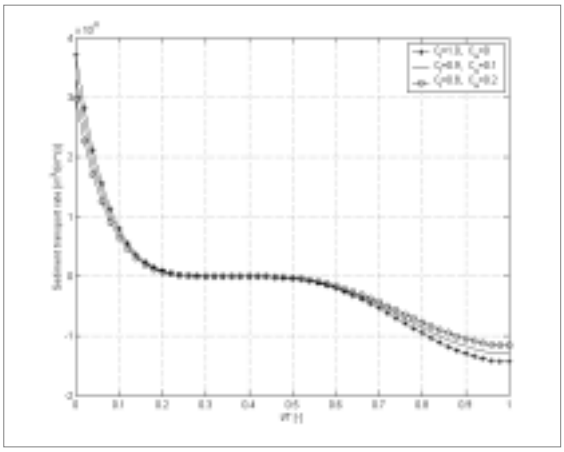

Figure 4-2a*, Lower layer transport rates for varying contribution coefficients at water depth 0.038[m].*

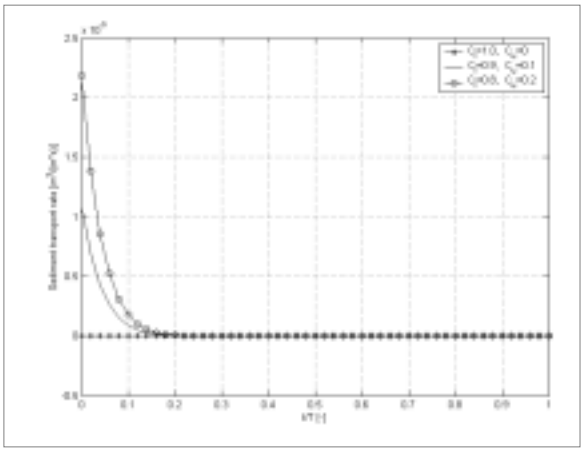

Figure 4-2b*, Upper layer transport rates for varying layer layer contribution coefficients at water depth 0.038[m].*

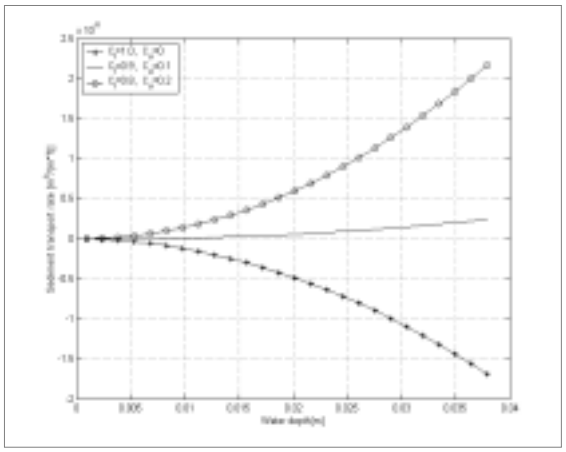

Figure 4-3, *Net sediment transport rates along the beach profile for varying layer contribution coefficients*

Looking at the intra wave sediment transport rates, figures 4-2a and 4-2b show a large increase of the sediment transport rate in the upper layer for a increase of the upper layer contribution coefficient, C_u. The explanation for this can be found in the layer thickness and velocity distribution during the passing of the wave. In figure 4-4 and 4-5 the velocities and the intra wave height of the upper layer are plotted for a waterdepth of 0.038 *[m]*. The velocity in the upper layer starts at a high value when the bore passes and then rapidly decreases. This high value of the water velocity is responsible for a high value of the sediment transport rate in the upper layer when the bore passes. The thickness of the upper layer (bore height) rapidly decreases after the passing of the bore. The layer thickness is already of insignificant height when the velocity in the upper layer becomes negative.

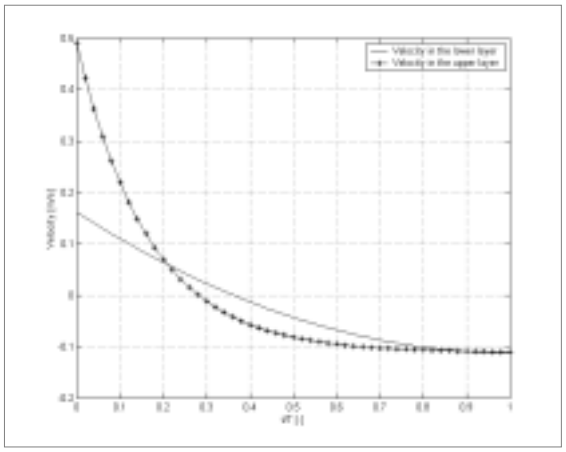

Figure 4-4, *Intra velocities on water depth 0.038 [m].*

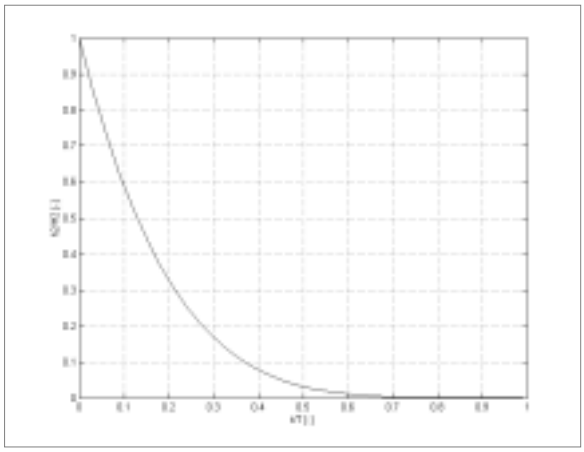

Figure 4-5, *Intra wave bore height*

Since the velocity and the upper layer thickness determine the sediment transport rate, this results in a large shoreward sediment transport rate for the upper layer.
Increasing the influence of the upper layer initially results in a decrease of the net seaward sediment transport. When the contribution of the suspended sediment transport in the upper layer is increased further, the net sediment transport rate changes from seaward to shoreward.

The intra wave plots, figure 4-2a and 4-2b show that the intra wave sediment transport rates (the solid line) are in the order 10 times larger than the net transport rates. This means that small changes on the intra wave sediment transport process for these settings have significant influence on the net sediment transport rate.

Simulations for a range of values for the upper and lower layer contribution coefficient have been conducted. The ratio between the upper and lower layer however is held constant through the inner region for each simulation.
In reality however, the sediment concentration in the upper layer will decrease when the water depth increases, so the influence of the upper layer is assumed to decrease when the water depth increases. This suggests that the ratio between upper and lower layer contribution coefficient changes through the inner region. In paragraph 5.1 this will be discussed.

4.2 The influence of the friction factor

The friction factor, f_w used in the ISZ-sediment transport model to determine the fluid power, P, is described by Bagnold (1963; 1966), chapter 3. Puleo and Holland (2001), found empirical values for the friction factor during their field measurements. They observed that the friction factor changes in time.
According to Puleo and Holland (2001) the friction factor changes through the tidal cycle and is different for uprush and backwash. Their field investigation shows that the friction factor for the uprush is constant over the swash cycle and can be set to 0.005-0.01. The backwash friction coefficient however was found to be up to three times larger than the uprush friction factor.
The backwash friction values range from 0.01-0.03 and depend on the tidal cycle, with the large values belonging to eb tide.
The range of friction factor values found by Puleo and Holland (2001) are illustrated (figures 4-6 and 4-7) and the changes on the sediment transport rates are discussed. The values calculated by Bagnold's method (1963;1966), (see paragraph 3.2.5) are well within the range of the values found in the field.

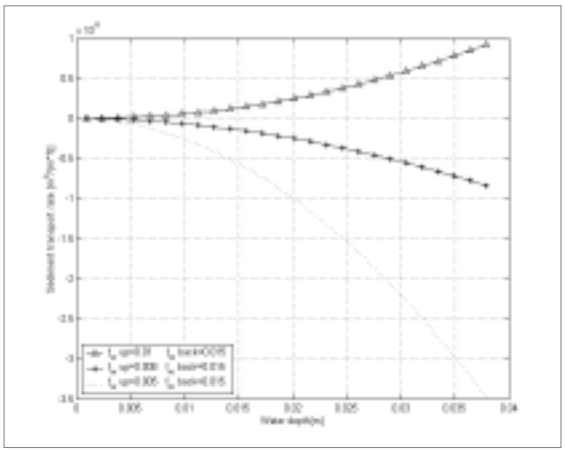

Figure 4-6, *Net sediment transport rates for varying friction in the uprush.*

Table 4-2, *Values for the friction factor, varying in the uprush.*

Simulation	Uprush, f_w	Backwash, f_w	Ratio $[f_{w\,up}/f_{w\,back}]$	Line
4	0.01	0.015	0.66	Δ
5	0.008	0.015	0.53	*
6	0.005	0.015	0.33	…

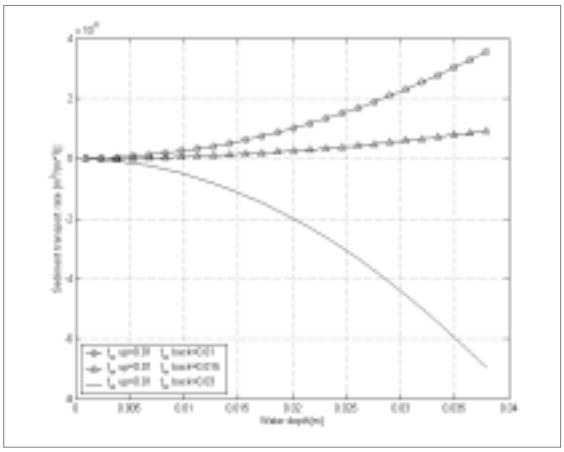

***Figure 4-7**, Net sediment transport rates for varying friction in the backwash*

***Table 4-3,** Values for the friction factor, varying in the backwash.*

Simulation	Uprush, f_w	Backwash, f_w	Ratio $[f_{w\,up}/f_{w\,back}]$	Line
7	0.01	0.010	1	o
8	0.01	0.015	0.66	Δ
9	0.01	0.030	0.33	-

Simulations 4 (Δ) and 8 (Δ) have the same settings and can be used as reference when comparing plots 4-6 and 4-7. Simulations 6 (dashed line) and 9 (solid line) have the same ratio between uprush and backwash. Both simulations show a net seaward sediment transport rate along the beach profile, however the magnitude of the sediment transport rate differs a factor 2. This indicates that the ratio between uprush and backwash is no basis for valid conclusions. The sediment transport can easily be set from extreme shoreward to extreme landward values by changing the friction factor. Choosing the right balance between uprush and backwash can lead to an equilibrium, a zero net transport situation.

4.2.1 Important factors on the friction factor used here

The friction factor has significant effect on the sediment transport rate. The friction factor itself is continuously influenced. These influences will be shortly mentioned here:

- During the uprush the leading edge of the uprush is not hindered by fluid landward of it. However during the backwash the flow can't flow freely under gravity and friction since the backwash is hindered by the fluid mass offshore.

- Nielsen (1992) showed that the shear stress increased for accelerating flows and decreased for decelerating flows in comparison to free stream velocities. So the accelerating backwash flow will cause an increasing shear stress and the decelerating uprush will cause a decreasing shear stress.

- Beach permeability allows vertical fluid transport through the beach influencing the bed shear stresses. Swash infiltration would increase the shear stress and the bed, while exfiltration would decrease the shear stress on the bed Oldenziel and Brink (1974); Conley and Inman (1994;).

- The vertical transport of the fluid through the beach can be increased by rainfall, this will cause increasing shear stresses.

The influences described here on the friction factor, cause a continuos varying friction value and makes it difficult to determine the right value for the friction factor.

4.3 Influence of the bed load/suspended load

Research on the swash zone by Horn and Mason (1994) and Masselink and Hughes (1998) shows that bedload (sediment load in the lower 0.01m of the water column) is significant and might even dominate the backwash. During the uprush, suspended load is significant and can dominate the sediment transport process, particularly when the uprush is bore initiated.

Bailard (1981) introduced the bed load and suspended load efficiency factor in his energy based sediment transport model. These efficiency factors resemble the contribution of the bed load and suspended load to the sediment transport rate.
The influence of the bed load and suspended load can be varied in the ISZ-sediment transport model by adjusting these bed load efficiency factor, ε_b and suspended load efficiency factor, ε_s (see equations 3-3 and 3-4). The values of the efficiency factors, ε_b and ε_s are estimated by Bailard (1981), determined a 95% certainty range for the bed load and suspended load efficiency factor based on field and laboratory data. Using the least square error method he found 0.21 for the bed load efficiency and 0.025 for the suspended load efficiency, these values are used in Bailard's energy based sediment transport model. The 95% confidence bounds on ε_b and ε_s are $0 < \varepsilon_b < 0.44$ and $0.016 < \varepsilon_s < 0.031$.
Figure 4-8 shows the influence on the transport rates, while varying the bed load efficiency factor, within the 95% confidence bounds.

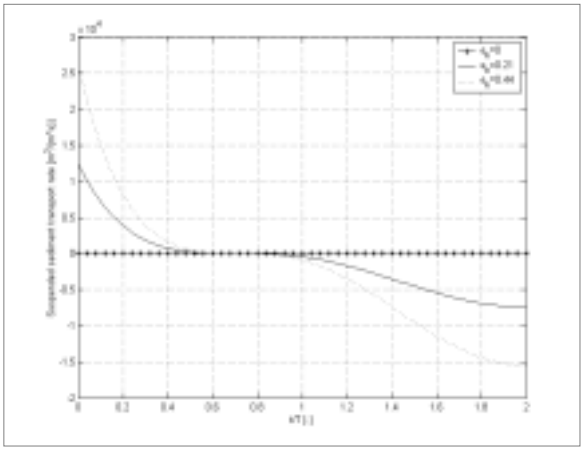

Table 4-4, *Values for the bed load efficiency.*

Simulation	Bed load efficiency factor, ε_b	Line
10	0	*
11	0.21	-
12	0.44	..

Figure 4-8, *Intra wave sediment transport, on water depth 0.038[m] for changing bed load efficiency,* ε_b.

As can be seen, the intra wave sediment transport rates for the bed load changes significant while varying the bed load efficiency factor, ε_b. A decreasing bed load efficiency factor, ε_b results in a decrease of the bed load transport. Changing the efficiency factor for the suspended load, ε_s within the 95% confidence bounds determined by Bailard (1981), hardly influences the intra wave suspended load transport rates. The net transport rates however do show variation while varying the suspended load efficiency coefficient. This once more confirms the sensitivity of the net sediment transport rates to small changes in the intra wave sediment transport.
The influence on the net sediment transport rate for varying the bed load and suspended load efficiency factors is illustrated in figure 4-9 and 4-10.

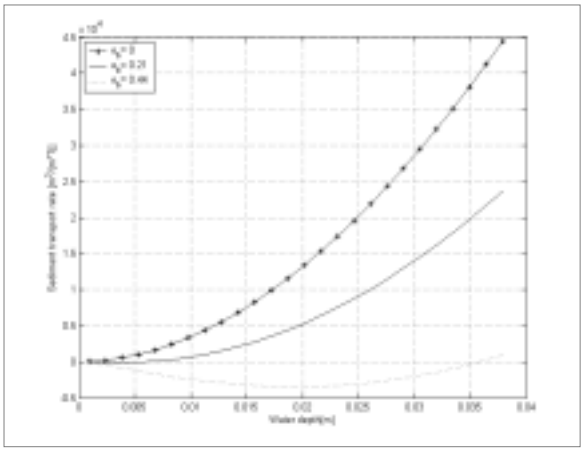

Table 4-5, *Values for the bed load efficiency factor.*

Simulation	Bed load efficiency factor, ε_b	Line
10	0	*
11	0.21	-
12	0.44	..

Figure 4-9, *Net sediment transport along the beach profile for changing bed load efficiency factor, ε_b.*

As can be seen the net sediment transport rates change significant while varying the bed load efficiency factor within the 95% confidence bounds determined by Bailard (suspended load efficiency factor is constant, 0.025). The net sediment transport rate even changes from shoreward to seaward. The bed load efficiency factor has significant influence on the net sediment transport rate.
In figure 4-10 the net transport rates along the beach profile are plotted while varying the suspended load efficiency factor within the 95% confidence bounds. The bed load efficiency constant, 0.21 (value found by Bailard). Simulations 11 and 14 have the same settings and can be used as a reference in plots 4-9 and 4-10.

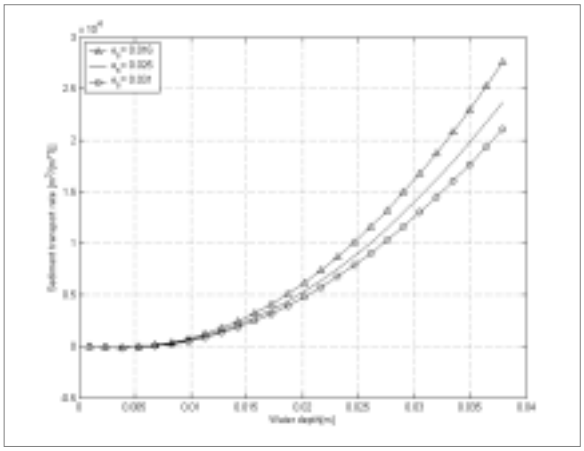

Table 4-6, *Values for the suspended load efficiency.*

Simulation	Suspended load efficiency factor, ε_s	Line
13	0.016	Δ
14	0.025	-
15	0.031	o

Figure 4-10, *Net sediment transport along the beach profile for changing suspended load efficiency factor, ε_s.*

Changing the suspended load efficiency, ε_s within the 95% bounds does not effect the net sediment transport rates along the beach profile as much as varying the bed load efficiency factor, ε_b. However the net transport decreases significantly when the suspended load efficiency factor increases.

Varying the efficiency factors can be used when the conditions change for example when the swash becomes bore initiated and the suspended load becomes dominant in the uprush. Or when the sediment composition changes from quartz to heavy minerals and the bed load transport becomes more important.

4.4 Conclusions

- A small change in the layer contribution coefficients, C_u and C_l changes the net sediment transport along the beach dramatically. Increasing the contribution factor, C_u for the upper layer decreases the seaward sediment transport initially and when increased further it results in a shift from seaward to shoreward net sediment transport.

- The intra wave sediment transport is considerably larger than the net sediment transport rate. This makes the ISZ sediment transport model sensitive in this range for small changes of the process parameters discussed above. Small modifications on the intra wave sediment transport process leads to large influence on the net transport rate.

- The friction factor, f_w incorporates many processes. These processes, cause a continuous varying friction value and make the friction factor's value difficult to compute.

- Changing the bed load efficiency, ε_b within the 95% confidence bounds has significant influence on both the intra wave sediment transport rate as the net sediment transport rate.

- The suspended sediment transport rates show no significant changes within the 95% confidence bounds on the variation of the suspended load efficiency factor, for the intra wave sediment transport rates. The net sediment transport rates however show significant changes when the suspended load efficiency factor is varied. This confirms the sensitivity of the net sediment transport rates to small intra wave sediment transport changes.

5 Calibration and Validation

The ISZ-sediment transport model presented in chapter 3 is calibrated against the data of Koomans, 1998. The experiments of Koomans (2000) are for spilling breaking. The tests of Koomans are in the same spilling breaking range as the experiments done by Stive (1980). These tests done by Stive (1980) form the base of the inner surf zone model, Aarninkhof (1999) (see paragraph 2.3.2). The process parameters friction, f_w and layer contribution, (C_l and C_u) discussed in chapter 4 are used for calibration.
After the calibration the model's behaviour is tested against varying field conditions (wave period, wave height, grain density, grain size and beach slope). The results of these test are compared with the findings of Kroon (1994), Koomans (2000), May (1973), Dubois (1972) and Puleo et al. (2000) and a suggestion is made how to vary the friction coefficient, the layer contribution coefficients or bed/suspended load efficiency factors to obtain a good match between model prediction and field observation.

5.1 Calibration to Koomans

Although wave flume experiments are a simplification of the sediment transport processes in nature, the ISZ sediment transport model is tested against the experiments of Koomans in the Scheldt flume of Delft Hydraulics, 1998. In figure 5-1 the layout of the experiment in the Scheldt flume can be seen. The locations of the wave height meters (WHM) and positions of measuring verticals (vertical dashed lines) are indicated.
In these experiments Koomans investigated sediment transport and density sorting in the cross section of the surf zone. The test used for calibration (A100-106) contains only quartz, used by Koomans as reference for his other test series, containing heavy mineral mixtures.

Settings Koomans, Series A100-106:

- *Beach slope, plane tan β =0.025* *[-]* *(slope 1:40)*
- *Wave height, H_s=0.12* *[m]*
- *Wave period, T_p =2* *[s]*
- *Quartz sediment composition, ρ =2430* *[kg/m^3]*

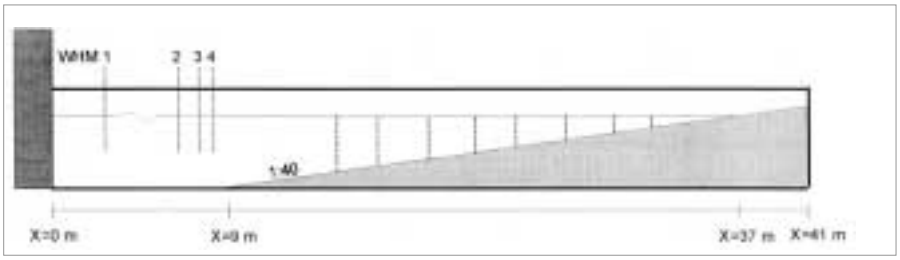

Figure 5-1, *Schematic set up of Kooman's experiment in the Scheldt flume.*

Although the conditions Koomans used are storm conditions, the breaking is still spilling.
The ISZ model, Aarninkhof, 1999 was tested against the tests of Stive (1980), paragraph (2.3.2). These tests were in the range of spilling breaking. The ISZ sediment transport model, based on the ISZ model is calibrated against the tests of Koomans, spilling breaking (see table 5-1).
So the ISZ sediment transport model will also be valid for spilling breaking.

Table 5-1, Settings *the tests of Stive and Koomans and their Irribarren parameter*

Parameter	H_s	$T_{wave\ maker}$	H_0/L_0	Irribarren, ζ	Breaker type
Test 1 (Stive)	0.178	1.79	0.032	0.140	Spilling
Test 2 (Stive)	0.226	3.00	0.010	0.257	Spilling
Koomans	0.120	2.00	0.027	0.180	Spilling

5.1.1 Calibration parameters

The process parameters, friction, f_w and layer contribution coefficients C_u, C_l for the upper and lower layer respectively are used for calibration. The range of these parameters is discussed in the previous chapter. The friction parameter for the uprush is assumed to be constant, $f_w = 0.01$ *[-]*, according to Puleo and Holland (2001). For the friction factor in the backwash the $f_w = 0.0163$ *[-]* was found (calibration value). The values for the friction coefficient lay well in the range of the values Puleo and Holland (2001) found.
The layer contribution coefficients, C_u and C_l initially have constant values, C_u=0.1 and C_l=0.90 for the upper and lower layer respectively.
In figure 5-2 the calibration against the data of Koomans (2000) is illustrated.

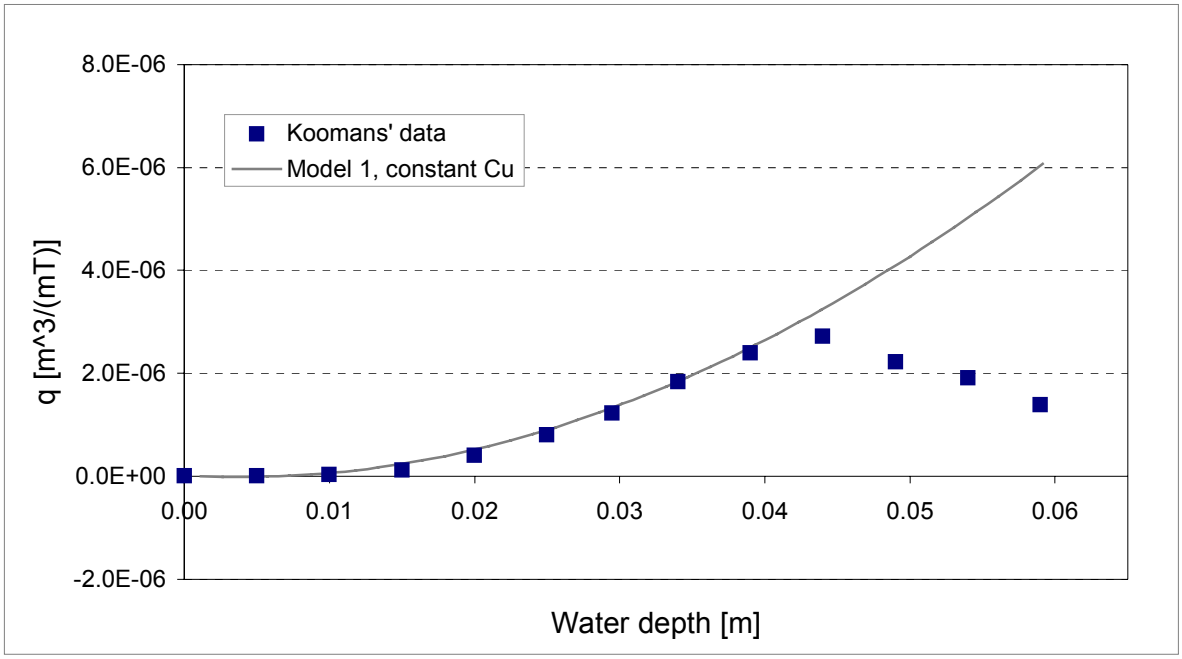

Figure 5-2*, Calibration to Koomans*

The data points of the experiments of Koomans and the model curves computed by the ISZ sediment transport model match quite well from 0 to 0.04 [m]water depth.
The "model 1" line with constant upper layer contribution coefficient, C_u fails when the water depth exceeds 0.04 [m].

It can be assumed that the contribution of the upper layer in deeper water is small and increases as the water depth decreases (see paragraph 4.1), due to the increasing sediment concentrations in the upper layer for decreasing water depth.

This water depth dependent influence of the upper layer on the sediment transport can be described by an empirical function (equation 5-1). This function resembles the increasing contribution coefficient for the upper layer when the water depth decreases. The values of the presented coefficients in this empirical formula are determined when the results presented in figure 5-2 are calibrated against the data of Koomans (see figure 5-4).

$$C_u = 0.05 \cdot C_u^* \cdot \left(1 + \tanh(0.223 \cdot T_{nl} - 4.7)\right) \qquad \textbf{Equation 5-1}$$

In which:

- T_{nl} *: The dimensionless non linearity parameter (equation 2-1).* *[-]*
- C_u^* *: The maximum value for the upper layer contribution coefficient, 0.10.* *[-]*
- C_u *: The depth dependent value for the upper layer contribution coefficient.* *[-]*

T_{nl}, the non linearity parameter depends on the water depth and the wave peak period see equation 2-1. The T_{nl}, non linearity parameter is dimensionless.

The value for the lower layer contribution coefficient is automatically corrected, by the expression (5-2) for lower layer contribution coefficient, C_l.

$$C_l = (1 - C_u) \qquad \textbf{Equation 5-2}$$

The empirical formula 5-1 is plotted in figure 5-3. On the x-axis the depth dependent non linearity parameter, T_{nl} can be seen. On the y-axis the values for C_u, the depth dependent upper layer contribution coefficient is plotted.

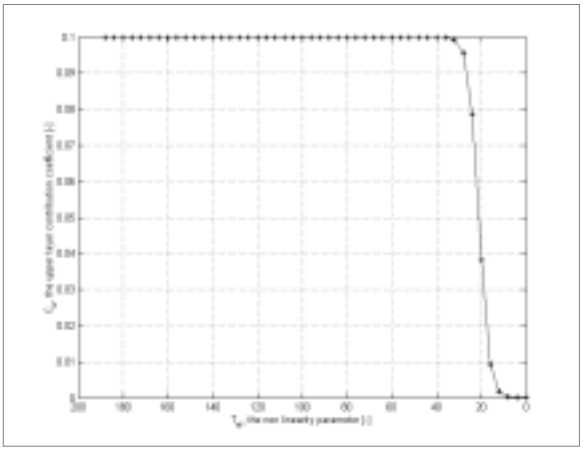

Figure 5-3, *Formula for the upper layer contribution coefficient, C_u*

For small water depths the value of the non linearity parameter is high, representing the high non linearity of the waves. The water depth dependent contribution coefficient of the upper layer, C_u reaches its maximum value of 0.10 for small water depths. When the depth decreases, the non linearity parameter, T_{nl} increases and when it reaches the value 30, the influence of the upper layer rapidly decreases. On larger water depths the value of the non linearity parameter T_{nl} rapidly approaches zero. The value of the upper layer contribution coefficient, C_u also approaches zero and hardly changes anymore (the line becomes horizontal). This however is beyond the validity of the ISZ sediment transport model.

The point were the influence of the upper layer rapidly increases, $T_{nl} = 30$ is the point were Unibest-TC ceases computations.

The graph (figure 5-4) shows the calibrated line of the ISZ sediment transport model to the tests performed by Koomans (2000). The grey coloured "model 1" line refers to the initial setting with a constant value for the upper layer contribution coefficient ($C_l = 0.9$ and $C_u = 0.1$). Using the depth dependent upper layer contribution formula (5-1) the baseline is replaced by the dark "model 2" line. The blocks refer to Koomans' data.

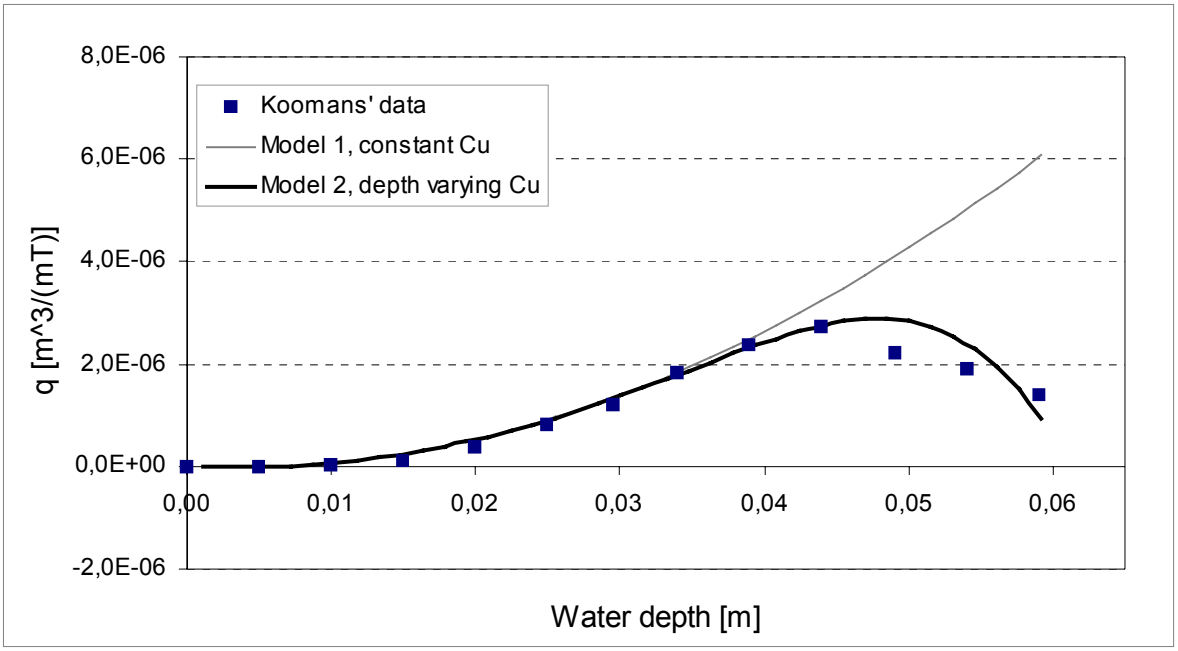

***Figure 5-4**, Calibration to Koomans*

The data points of the experiments of Koomans (figure 5-4) and the model curves computed by the ISZ sediment transport model match quite well up to 0.04 [m]water depth.
As can be seen the "model 2" line, with depth varying C_u fits the data points of Koomans up to 0.065[m] water depth. So using the calibrated empirical formula 5-1, for decreasing influence of the upper layer in sediment transport when the water depth increases, extends the model's range.

5.1.2 Validity

The ISZ sediment transport model is valid for spilling breaking and uses two boundaries.
A seaward boundary, determined by the non linearity parameter, T_{nl} and a shoreward boundary, where the waterdepth is zero. These two boundaries refer to the starting point and the endpoint of the computations of the ISZ-sediment transport model.

Seaward boundary

To determine the starting point of the ISZ sediment transport model's computations, the non linearity parameter, T_{nl} (introduced in paragraph 2.1) is used. The T_{nl} is initially set to 30, which causes the model to start computations at waterdepth 0.7*[m]*-0.04*[m]* for wave periods from 8 *[s]* to 2 *[s]*.
However the model validity can be extended when the decreasing influence of the upper layer on the sediment transport for increasing water depth is taken into account (see figure 5-4).

This can be done by using the calibrated empirical function 5-1 for the upper layer contribution coefficient, C_u. Doing so, the starting point value for computations T_{nl} decreases from 30*[-]* to 24*[-]*. This is illustrated in figure 5-5.

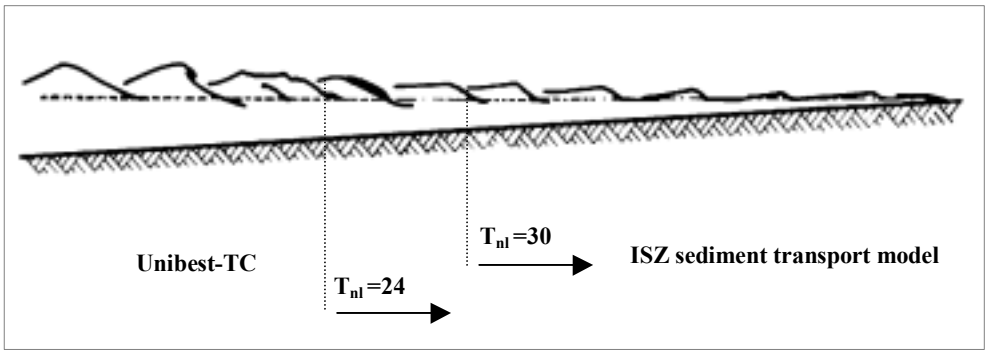

***Figure 5-5**, schematic review of the starting point of computations.*

For the wave period used by Koomans T= 2*[s]* this results in a extension of the validity of the ISZ sediment transport model from 0.04*[m]* to 0.065*[m]* water depth. For field conditions with wave periods up to 8 seconds this results in an extension of the validity of the ISZ sediment transport model from 0.7*[m]* to 1.1*[m]* water depth.

Shoreward boundary

The tests performed by Koomans show a zero transport at cross-shore position X = 38.5*[m],* indicating zero meter waterdepth on this point. Running the ISZ-model with the same settings yields a shoreward endpoint for computations, indicating to zero meter water depth at the same X-position. So the ISZ-sediment transport model resembles the sediment transport up to the same zero meter water depth location as found by Koomans in his test. This indicates that the ISZ model by Aarninkhof (1999) has computed the setup correctly.

5.2 Model response to changing field conditions

The behaviour of the model is reviewed here. The parameters (wave height, wave period, grain size/density and beach slope) are reviewed and their influence is tested. The influence of these parameters is reviewed in literature. Based on the findings in literature it is suggested to adjust the model parameters, friction (f_w) and bed/suspended load efficiency factor (ε_b, ε_s) under changing field conditions.
The outlined text describes the founding from literature

5.2.1 Wave height

The ISZ-sediment transport model is tested on its sensitivity to variable wave height.
The wave height is varied in the in the range of 0.17*[m]*-0.25*[m]*. Increasing the wave height moves the point of zero meter water depth onshore in the ISZ model, indicating more wave set up. The sediment transport related to the water depth shows no changes, however the local waterdepth increases and so does the sediment transport rate on that location. Stive (1980) mentions that the wave shapes propagating onshore are highly similar and the water motion on each point is strongly locally controlled. The ISZ model based on this similarity gives an equal sediment transport over the waterdepth, due to this locally controlled water motion.

The data from Egmond, (Kroon, 1989 and 1990) show that the local suspended sediment fluxes show an increase of the mean and net transport with increasing local relative wave height.
In case of non-breaking and spilling waves the local net fluxes are small.
However Kroon found that with increasing local relative wave height H_s/h, the suspended sediment transport becomes more important and might become dominant over the bed load transport.

Kroon also found that low to average energy wave conditions (offshore wave height less than 1*[m]* and local wave heights at the inner nearshore bar smaller than 0.4*[m]* during the flood period) leads to an accreting beach.
The moderate to high-energy wave conditions (offshore wave heights exceed 1 *[m]* and the local relative wave heights at the inner nearshore bar are in between 0.4*[m]* and 0.8*[m]* during the flood period) leads to an eroding beach.

So the sediment transport changes from accretion to erosion for increasing wave heights with the suspended sediment having significant contribution.
The ISZ sediment transport model shows an increase of the local sediment transport rate when the wave height increases, however this is due to an increase of the computed local waterdepth. Changing the bed load and suspended load efficiency factors, ε_b and ε_s respectively introduced by Bailard (1981), (see paragraph 4-3) with the changing wave height can resemble the findings of Kroon (1989 and 1990). For increasing wave height the suspended load efficiency factor can be increased, resembling the higher fluxes. A decreasing wave height requires the opposite. Increasing the suspended load efficiency factor also leads to a decrease of the onshore sediment transport rate (see paragraph 4.3). Indicating a decrease of accretion and when the suspended load efficiency factor is increased further, the model will show offshore sediment transport, indicating erosion, for the settings presented here.

5.2.2 Wave period

On the influence of the wave period on the sediment transport fluxes the findings in the field described by Kroon (1989-1990) and Puleo (2000) differ.

A study of swash zone sediment transport was conducted at Glendon Beach, Oregon during February, 1994. The influence on the sediment transport is described by Puleo et al. (2000). Measurements were performed on swash events of different duration. The suspended sediment concentrations through time were measured. The concentrations of the suspended sediment are equal in the range of 1-3 *[cm]* above the bed for the different events. In the rest of the range of the measurements the suspended sediment concentration shows a correlation with the duration of the event.
In all cases the uprush is characterised by high suspended sediment concentrations at t=0, the passing of the bore. The suspended sediment concentration then rapidly decreases as the swash front passed the sensors.
The backwash suspension is different from the uprush suspension. In all cases the uprush suspended sediment concentrations are a factor 2 up to 7 larger than the backwash suspended sediment concentration. The suspended sediment concentration for the backwash also increases with the swash event duration. The net swash duration was always onshore for the three events and the net onshore transport decreased with the increasing duration of the swash events.

The measurements of Kroon in the field, Egmond (1989-1990) for wave periods varying from 3*[s]* to 13*[s]* (spilling to plunging bores) do not confirm to what Puleo et al found.

Kroon found that the wave peak period has no significant correlation with the net suspended sediment transport rate.

In figure (5-6) the intra wave suspended sediment transport rate is illustrated. The plot is at waterdepth 0.038 *[m],* and the settings are according to Koomans' calibration.

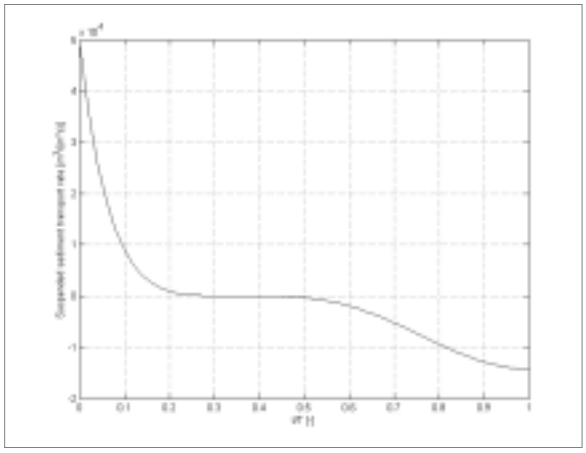

Figure 5-6, *Suspended sediment transport rates for T=2[s] and waterdepth 0.038 [m].*

In this intra wave suspended sediment transport rate plot the first part can be considered to be the uprush, where the sediment transports are high and shoreward. The last part, where the sediment transport is seaward can be considered as the backwash. It can be seen that the sediment transport rates in the first part are a factor five larger than the transport rates in the backwash. This is in agreement to what Puleo (2000) found.

Increasing the wave period does not result in a higher net suspended sediment transport rate in the model. This is not in correspondence to what Puleo (2000) described, however it is according to what Kroon (1989-1990) found.
Since there is no agreement on this point no recommendations will be made to adjust the model's parameters friction (f_w), bed/suspended load efficiency factor (ε_b, ε_s) or layer contribution coefficients (C_l and C_u) to represent changes in sediment transport for changing wave period.

5.2.3 Grain density/size

The grain density and the grain size are reviewed in this paragraph. First a general description is given, followed by the model computations.

General
As the swash of the wave ascends the sloping beach, energy is increasingly lost, resulting in a decrease of the velocity to zero.
From this state of rest the water starts to flow back on the slope entirely driven by gravity.
The smaller grains accumulate in the slower moving water, and the larger ones in the faster moving water. This explains why the finer, or less dense grains can be found at the swash line where the water is stationary, or nearly so, while the coarser or denser grains can be found at the plunge line where the velocities are large (Evans, 1939).

In a wave field approaching the coast a selection of particle motion can be made in three classes (May, 1973):

1. **No motion**: the sediment particle is either too large, too dense or too sheltered to be moved by the maximum water velocities
2. **Unidirectional flow**: the sediment particle has such a size, position or density that it can be moved shoreward under the crest, but not moved seaward under the through.
3. **Bi-directional motion**: the sediment particle can be moved both shoreward and seaward under the flow circumstances.

Greater velocities than for quartz are required to transport the heavy minerals of a sediment population because:

- Heavy minerals generally fall into the finer fraction. Small grains are hard to entrain, because they tend "hide" behind the larger grains.
- They have a greater mass density.

Angle of the foreshore slope

A foreshore consisting of coarse material has a high rate of permeability, so that the energy component of the swash and particularly of the backwash is reduced. A reduction of the energy of the backwash leads to a steeper foreshore slope to establish an equilibrium between wave process and gravity, Dubois (1972).
When the particle size of the sediment composition decreases, the permeability decreases. This leads to an increase of the backwash, leading to a decrease of the foreshore slope.

Dubois (1972) found that increasing the heavy mineral content leads to a steepening of the foreshore slope, although increasing the heavy mineral contend leads to a decrease of permeability, since increasing the heavy mineral contend leads to a decrease of grain size. However the increase of heavy mineral content increases the weight per volume of the foreshore sediment, increasing the resistance to be removed by the backwash.
He found that the foreshore slope has a direct relation with the ability of sediments to resist removal, the increase of weight per volume overrules the decrease in permeability.

Conclusive

- Availability of heavy minerals decreases the transport rates since the heavy particles are harder to entrain, especially in the backwash.
- Coarser material on beaches leads to steeper equilibrium profiles, since the backwash energy is reduced.
- Availability of heavy minerals leads to steeper equilibrium beach profiles, since the velocities in the backwash are not large enough to transport the heavy particles.

Density

Koomans found (2000) found a higher volumetric sediment transport rate per time interval for the quartz bed composition, in comparison with the zircon quartz mixture bed composition in his tests.

The model's behaviour on changing the density of the grains is illustrated in figure 5-7.
The solid line refers to the condition with a quartz bed composition. The stars-marked line refers to a condition with a heavy mineral bed composition. For both simulations the calibration values discussed in paragraph 5.1.1 are used.

The specific qualities of the heavy minerals are:

- *Grain size* d_{50}= 115, d_{90}= 153 [μm]
- *Fall velocity* w_{s50} = 0.027 [m/s]
- *Density* ρ = 4400 [kg/m^3]

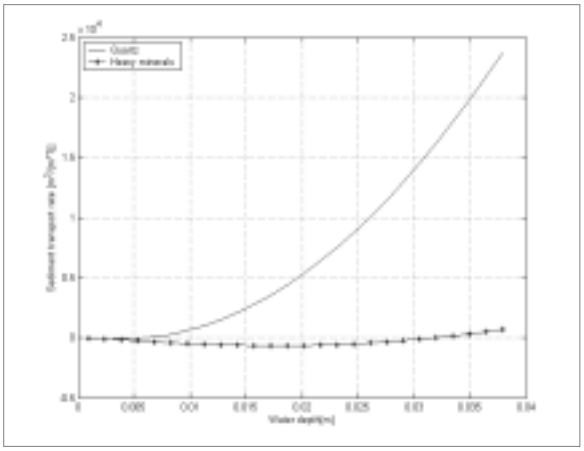

***Figure 5-7**, Sediment transport rates along the beach profile, for quartz (-) and heavy minerals (*)*

The model shows a similar trend to what Koomans found, however the model shows a small negative value for the first region.
This is caused by an overestimated role of the backwash when using a heavy mineral bed composition, changing the sediment transport rate from shoreward to seaward.
To eliminate this overruling backwash transport a decrease of the friction factor for the backwash is required, this compensates the backwash overestimation. Decreasing the friction factor for the backwash will also result in a steeper foreshore equilibrium profile, which is according to what Dubois found (1972).

According to the theory of May (1973), "a selection of particle motion"(see above) one should expect mainly transport during the passing of the bore, since the velocities are relatively high during this passing. In the backwash, the velocities are smaller and it is possible that the heavy minerals will not move under these circumstances. The model uses the energy approach of Bailard (1981) and show movement of the grains under all circumstances. This implies that the selection by May (1973), made for the grain movement, is ignored in the ISZ sediment transport model. To take the beginning of movement of a grain into account, one should use a Shield based sediment transport model. Shields describes the beginning of movement of a grain, see appendix A.

Furthermore the suspended load contribution is assumed to decrease for increasing density, so the efficiency factor, ε_s for the suspended load (see paragraph 4-3) must be decreased, resembling the influence of the increased density on the sediment transport.

Grain size

In coastal morphology one of the fundamental facts is the relation between foreshore slope angle and grain size, see "angle of the foreshore slope" above. For a given wave energy, the coarser the material, the steeper the foreshore slope becomes to establish equilibrium between waves and gravity.

The model's behaviour on changing the grain size is illustrated in figure 5-8 for the grain sizes listed in table 5-1. During the simulations, the calibration values discussed in paragraph 5.1.1 are used.

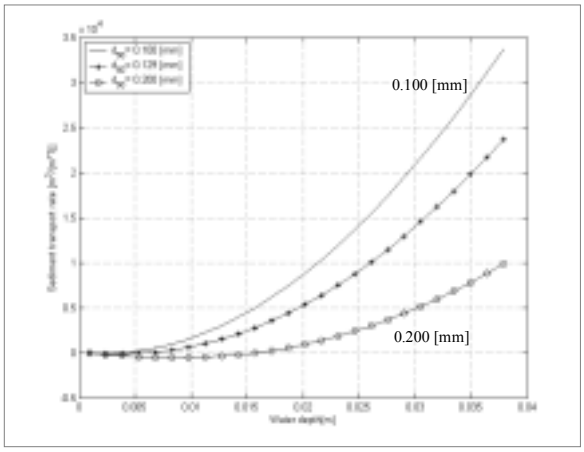

***Figure 5-8**, Sediment transport rates along the beach profile, for different grain sizes.*

***Table 5-1,** The used different grain sizes*

Grain size, d_{50} [mm]	Fall velocity [m/s]	Line type
0.100	*0.009*	*
0.129	*0.012*	-
0.200	*0.019*	*o*

The ISZ sediment transport model shows a decreasing shoreward transport for the larger grains sizes, however the beach is still accreting. The decreasing sediment transport, in the ISZ model is due to the higher fall velocities of the larger grains.

Increasing the friction factor for the backwash by increasing grain size would give a increasing sediment transport in the backwash, resulting in a smaller (or even negative) net sediment transport.
Increasing this friction factor with increasing grain size will also lead to an steeper equilibrium profile here. This is according to what was found by Dubois (1972).

5.2.4 Beach slope

The field measurements by Kroon (1989, 1990) on sediment transport and morphodynamics of the beach and nearshore zone near Egmond, showed that the beach slope is changed under changing energy conditions. These energy conditions depend on the wave heights. When the significant wave height is large, the energy conditions are high. The beach research near Egmond yielded that when going from moderate to high energy condition, the beach changes from accretion to erosion. The beach changes from steep, an angle of 7 degrees to mild, an angle of 2 degrees. This is according to the description of the summer and winter profile developments as described by Van der Velden (1989). In the summer the wave height decreases, the wave period normally increases and the sediment transport becomes shoreward, the beach is accreting, in the winter the opposite occurs. The summer profile is steeper than the winter profile.

The beach changes continuously trying to reach the equilibrium beach profile. The real equilibrium beach profile is never reached, a dynamic equilibrium exists. Officially the beach slope is not a parameter that can be varied, since it is a reaction on the wave height and the grain size/density. However towards a better understanding of the beach slope development, different angles are tested in the ISZ-sediment transport model.

In the ISZ sediment transport model different beach angles are inserted and the sediment transport rates, belonging to these angles are computed and plotted (see figure 5-9). The

simulated beach angles and their breaker types are listed in table 5-2. In all the simulation the calibration values found in paragraph 5.1.1 are used.

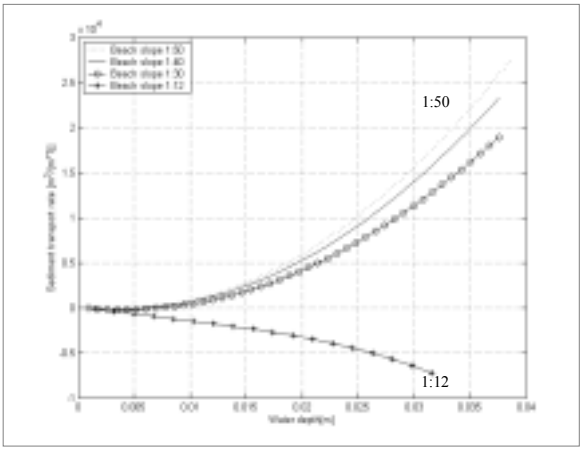

Figure 5-9, *Sediment transport rates belonging to different beach profiles.*

Table 5-2, *Summary of the modelled beach slopes*

Beach slope	Line type	Breaker type
1:50	..	*Spilling*
1:40	-	*Spilling*
1:30	*o*	*Spilling*
1:12	*	*Spilling*

The transport rates computed by the ISZ-model show the influence of a steeper beach profile in a reasonable way. The beach slopes presented here are all not in equilibrium, since the net transport rates are non-zero.
When the beach slope decreases the onshore sediment transport increases, indicating to an accretion state of the beach here. When accretion takes place in nature, the beach slope increases until an equilibrium profile is reached.
A milder beach slope indicates to erosion in the field, the model computes offshore transports on a steep beach slope, indicating a non-equilibrium beach profile. The beach profile will erode to a milder profile until equilibrium is reached.

5.3 Conclusions

- Increasing the influence of the upper layer, representing the increasing sediment concentrations in the upper layer for decreasing water depth, extends the range of the ISZ sediment transport model significantly.

- The local sediment transport rates increase for increasing wave height. To resemble the other effects of changing wave conditions the suspended and bed load coefficients, ε_s and ε_b can to be adjusted in the ISZ sediment transport model.

- When the sediment composition changes the model provides reasonable results. When necessary the friction factor in the model can be adjusted to obtain the correct sediment transport rates of the ISZ sediment transport model.

- The changes in sediment transport rates for varying beach slopes can encouraging well be predicted by the developed ISZ sediment transport model.

6 Conclusions and recommendations

First the conclusions on the thesis will be reviewed, followed by the recommendations for further research.

6.1 Conclusions

The goal of this thesis was to create a better understanding of the sediment transport processes of the inner surf-zone (ISZ) and the influence of changing field conditions on the sediment transport.
An ISZ sediment transport model was developed, which starts calculations were other sediment transport models like Unibest-TC cease them. The ISZ sediment transport model was calibrated against the data from the Scheldt flume (1998) by changing the friction factor and the layer contribution coefficients. From this thesis the following conclusions can be drawn:

- The net sediment transport is the integration of the intra wave sediment transport. Since the net sediment transport is an order of magnitude smaller than the intra wave sediment transport, the net transport rate computed by the ISZ sediment transport model is very sensitive to small changes in the intra wave sediment transport. Furthermore this implies that the net transport is only a small fraction of the sediment transported in a wave period.

- The bed load efficiency and suspended load efficiency factor, ε_b ε_s respectively introduced by Bailard (1981) in his energy based sediment transport model, can be varied over a range within 95% confidence bounds. Varying these efficiency factors, show a variation in the sediment transport rates. The changes in transport rate for varying the bed load efficiency in its range are larger than the changes found on the sediment transport when varying the suspended load efficiency factor. For changing wave conditions these efficiency factors can be adjusted, to represent the changes in transport fluxes.

- The friction factor, f_w, used in the ISZ sediment transport model to compute the shear stress, encompasses many uncertainties. Varying the friction over the range described by Puleo and Holland (2001) shows major changes in the sediment transport rates. The transport rates in this range vary from extreme shoreward values to extreme offshore values. Showing the significant influence of the friction on the sediment transport.
  The friction factor is used to calibrate the ISZ sediment transport model against the data of Koomans (2000). When the sediment composition of the bed changes, the sediment transport rates change. The friction factor can be adjusted to represent the changes for these changing conditions in sediment transport as described in literature.

- In the ISZ sediment transport model a separation of the sediment transport, into a upper and a lower layer is introduced. These layers have a layer contribution coefficient C_l and C_u for the lower and upper layer respectively, representing the contribution to the sediment transport in those layers. The ration between these coefficients is of major importance in regard to the sediment transport rates. Decreasing the influence of the upper layer for increasing water depth, representing the decreasing sediment concentrations in this layer, extends the range of the model significantly.

- The ISZ sediment transport model encouragingly well models the changing sediment transport rates for varying beach slopes, and varying sediment composition.

- For increasing wave height the ISZ sediment transport model shows increasing sediment transport rates for similar locations in the inner surf zone. This is due to the increasing water depth for increasing wave height on these locations, modelled by the ISZ. The sediment transport rates do not change for equal water depths.

- The ISZ sediment transport model uses Bailards energy approach to describe the sediment transport processes. The energy approach on sediment transport ignores the beginning of movement and so the ISZ sediment transport model will give transport rates under all circumstances even when the velocities are to small to transport the grains.

The ISZ model resembles the sediment transport rates reasonably well after calibration.
The changes to the sediment transport due to changing field conditions can be illustrated after tuning the process parameters, (friction and bed/suspended load efficiency factors). The model gives insight to the sediment transport processes in the inner surf zone, however the model requires detailed field descriptions to resemble the sediment transport rates in a reasonable way.

6.2 Recommendations

- Implementation of the developed ISZ sediment transport model with Unibest-TC. The sediment transport model Unibest-TC ceases computations at some distance before the shoreline. Creating a smooth transition between the developed ISZ sediment transport model and Unibest-TC results in a sediment transport model, which can compute the sediment transport rates from deep water up to zero meter water depth.

- The bed land suspended load efficiency factors, ε_b and ε_s respectively were varied within the 95% confidence bounds, showing significant influence on the net sediment transport rates. In the ISZ sediment transport model no difference was made in these coefficients between uprush and backwash. However the flow conditions in the uprush and backwash are quite different and so might the suspended and bed load contribution. Varying these efficiency coefficients over the uprush and backwash can represent these varying conditions.

- The energy approach Bailard (1981) used in the ISZ sediment transport model to compute the sediment transport rate, ignores the beginning of movement of the grains. Inserting Shields into the ISZ sediment transport model can represent this beginning of movement.

- The ISZ sediment transport model computes the sediment transport rates. These computed sediment transport rates can be used to determine the morphological changes of the beach profile, however when the beach profile changes so will the hydrodynamics.
  When the changes in beach profile are computed (for a small time window) the computations start again. Starting with determining the new hydrodynamics→ computation of the sediment transport rates→determining the morphological changes.
  Unibest TC can compute the morfological changes, so implementation with Unibest TC would provide a morfological model up to zero meter water depth.

7 References

Aarninkhof, S.G. J. and J.A. Roelvink, (1999) *Argus based monitoring of intertidal beach morphodynamics. Proc. Coastal sediments, New York: ASCE, pp2429-2444.*

Bagnold, R.A.,(1963) *Mechanics of marine sedimentation, in the Sea: Ideas and Observations, vol.3, Interscience, New York.*

Bagnold, R.A., (1966) *An approach to the sediment transport problem from general physics, U.S. Geol. Surv. Prof. Pap., 422-I.*

Bailard, J.A., (1981) *An energetics total load sediment transport model for a plane sloping bed, Journal of geophysical research, vol 86 pp.10.938-10954.*

Battjes, J.A., (1974) *Computation of Set-up, longshore currents, Run –up and overtopping due to wind-generated Waves. Dissertation Delft University of Technology.*

Battjes, J.A. and Janssen, J.P.F.M., (1978) *Energy loss and set up due to breaking of random waves, Proc 16 th Int. Conf on coastal Eng. Hamburg pp. 569-587.*

Battjes, J.A. and Stive M.J.F., (1985) *Calibration and verification of a dissipation model for random breaking waves. Journal of Geophysical Research 90, pp.9159-9167.*

Bosboom, J., S.G.J. Aarninkhof, A.J.H.M. Reniers, J.A. Roelvink and D.J.R. Walstra, (1997) *Unibest- TC 2.0. Overview of model formulations. Report H2305.42, WL Delft Hydraulics.*

Conley, D.C., Inman, D.L., (1994) *Ventilated oscillatory boundary layers, Journal of Fluid Mechanics 273 pp. 261-284.*

Dubois, R.N., (1972) *Inverse relation between foreshore slope and mean grain size as a function of the heavy mineral content, Geological Society of America Bulletin, Vol 83 pp. 871-876.*

Evans, O.F., (1939) *Sorting and transportation of material in the swash and backwash, Journal of Sedimentary petrology, Vol 9 pp28-31.*

Horn, D.P. and Mason, T., (1994) *Swash zone sediment transport modes. Marine Geology, 120, pp. 309-325.*

Hughes, M. and Masselink, G., (1998) *Field investigation of sediment transport in the swash zone Continental Shelf research 18 pp. 1179-119.*

Hughes, M. and Masselink, G., (1997) *Toward better understanding of swash zone sediment transport Coastal dynamics pp.805-813.*

Irribarren, (1938) *Una Formula para el Calculo de los Diques de Escollera. M. Bermejillo-Pasajes, Madrid, Spain.*

Koomans, R.L., (2000) *Sand in motion, effects of density and grain size.*

Kroon, A., (1994) *Sediment transport and morphodynamics of the beach and nearshore zone near Egmond, The Netherlands.*

May, J.P.,(1973) *Selective transport of heavy minerals by shoaling waves Sedimentology, 20 pp. 203-211.*

Oldenziel, D.M., Brink, W.E., (1974) *Influence of suction and blowing on entrainment of sand particles. Journal of the Hydraulic Division 100 (HY7), pp. 935-949.*

Puleo, J.A., R.A. Beach, R.A. Holman ans J.S. Allen, (2000) *Swash zone sediment suspension and transport and the importance of bore generated turbulence. J. Geophys. Res., Vol, No.C7, pp. 17,0 21-17, 044.*

Puleo, J.A. and K.T. Holland, (2001) *Estimating swash zone friction coefficients on a sandy beach, 2001. Coastal engineering 43 pp. 25-40.*

Schiereck, G.J., (2001) *Introduction to bed, bank and shore protection, pp.152-153.*

Stive, M.J.F., (1980) *Velocity and pressure field of spilling breakers, publication nr. 233.*

Stive, M.J.F. and De Vriend, H.J., (1994) *Shear stress and mean flow in shoaling and breaking waves. Proc. 24 th. Int. Conf. on Coastal engineering, New York: ASCE, pp. 594-608.*

Svendsen, I..A., (1984) *Wave heights and set up in a surf zone. Coastal Engineering 8, pp. 303-329.*

Svendsen, I..A., Madsen, P.A. and Buhr Hansen, J., (1978) *Wave characteristics in the surf zone. Proc.16 th Int. Conf. On Coastal Engineering, New York: ASCE, pp. 520-539.*

Thornton, E.B. and Guza, R.T.,(1983) *Transformation of wave height distribution. Journal of Geophysical Research 88, pp.5925-5938.*

Van der Velden, E.T.J.M. , (1989) *Coastal engineering volume II, Delft University of Technology, pp. 53 / 187-192.*

Yalin, M.S., (1977) *Mechanics of sediment transport, pp.117-122.*

Appendix A

The quartz and heavy sediment transport lines in the simulations approach the zero transport line for almost the same velocities, this once more implies that whether the grains can be moved or not is not taken into account.
The forces must form equilibrium under normal circumstances, to start moving, the driving force must exceed the gravity force, see figure1.
In the ISZ-sediment transport model uses the Bailard energy approach and doesn't take the phenomenon of beginning of movement into account. To do so a Shields approach must be introduced.

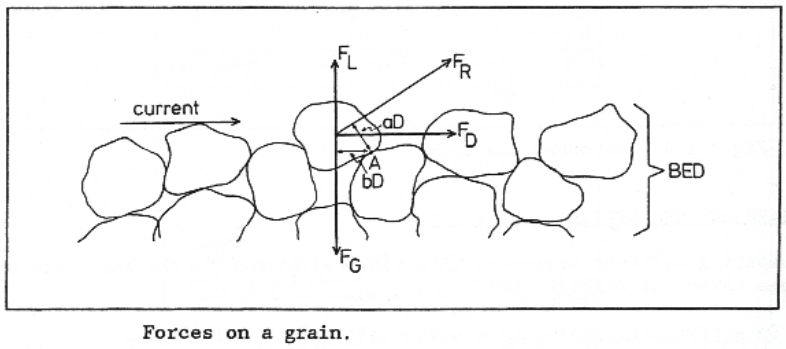

Figure 1

Shields denotes two phases for a grain:

- non-moving grains
- moving grains*, when Shield parameter exceeds value 0.03 (see figure 2)

In figure 2 the rest and movement areas for a grain are shown according to Shields.

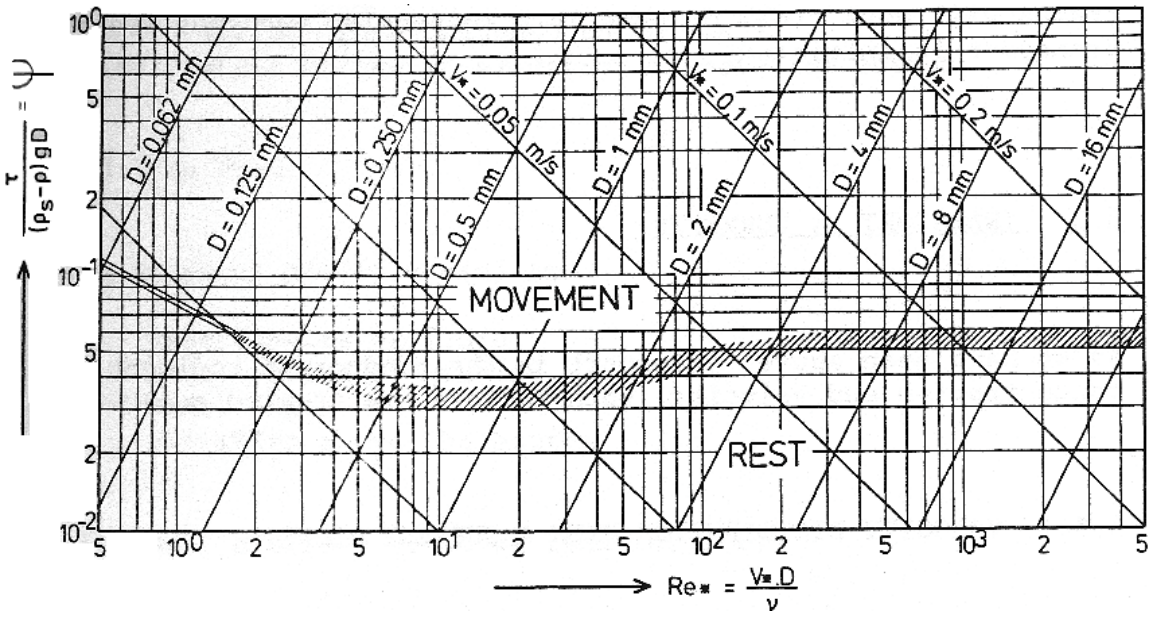

Figure 2